POLLUTION, DENSITY AND LOW EMISSION ZONES: EUROPEAN EVIDENCE

2026

BANCO DE ESPAÑA
Eurosistema

Documentos de Trabajo
N.º 2621

Nicolás Forteza and José M. Labeaga

POLLUTION, DENSITY AND LOW EMISSION ZONES: EUROPEAN EVIDENCE (*)

Nicolás Forteza (**)

BANCO DE ESPAÑA

José M. Labeaga (***)

UNIVERSIDAD NACIONAL DE EDUCACIÓN A DISTANCIA, SPAIN

(*) We are extremely grateful for Ana Pitarch's incredible research assistance. We also would like to thank an anonymous referee, Antonio M. Bento, Juan Pablo Montero, Federico Curci, Jordi Teixidó, Laura Rodríguez, Alberto Álvarez, Esteban García Miralles, Aitor Lacuesta and participants at the 10th Atlantic Workshop on Energy and Environmental Economics, Banco de España internal seminar, Universidad de Barcelona seminar, Université Catholique de Louvain, Saint-Louis, Brussels seminar, Annual Conference of the International Association for Applied Econometrics and International Panel Data Conference for their invaluable comments. The views expressed in this paper are those of the authors and do not necessarily represent the views of the Banco de España or the Eurosystem.
(**) nicolas.forteza@bde.es
(***) jlabeaga@cee.uned.es

Documentos de Trabajo. N.º 2621

July 2026

https://doi.org/10.53479/44145

ISSN: 1579-8666 (online edition)

Abstract

Low emission zones (LEZs) have emerged as a primary policy instrument to combat urban air pollution in Europe, yet rigorous evidence on their effectiveness and spatial spillovers remains limited. Using a high-resolution geospatial panel dataset covering 1km grid cells across 33 European countries from 2007 to 2022, we estimate that LEZ adoption reduces PM2.5 exposure by approximately 4% within designated zones. We find robust evidence of positive spillovers: pollution also declines in areas adjacent to LEZ boundaries. These average effects mask substantial heterogeneity: reductions are concentrated in larger, denser cities and in cities with medium-sized zones relative to total urban area, while the smallest cities and zones show no detectable effect. These findings suggest LEZs generate city-wide environmental benefits extending beyond formal boundaries, consistent with network effects and technology spillovers dominating displacement mechanisms. To contextualize these results, we estimate the pollution-density elasticity for European cities using instrumental variables based on historical settlement patterns, finding that a 1% increase in population density raises PM2.5 exposure by 6% (approximately half the magnitude documented for US cities). We interpret our findings through a spatial equilibrium model that formalizes how LEZs alter the pollution production function in monocentric cities. Our results indicate that moderate-stringency LEZs, as typically implemented across Europe, deliver meaningful aggregate pollution reductions of approximately 1.8% city-wide, with modal shift complementarities and fleet renewal mechanisms dominating traffic displacement effects.

Keywords: low emission zones, air pollution, PM2.5, urban density.

JEL classification: I10, Q53, Q58, R11, R12.

Resumen

Las zonas de bajas emisiones (LEZ, por sus siglas en inglés) se han consolidado como uno de los principales instrumentos de la política pública para combatir la contaminación del aire urbano en Europa. Sin embargo, la evidencia rigurosa sobre su eficacia y sus efectos espaciales sigue siendo limitada. Utilizando un conjunto de datos geoespacial de alta resolución que cubre celdas de 1 km² en 33 países europeos entre 2007 y 2022, estimamos que la adopción de las LEZ reduce la exposición a las partículas en suspensión con un diámetro de hasta 2,5 micras (PM2.5, por sus siglas en inglés) un 4 %, aproximadamente, dentro de las zonas designadas.

Encontramos evidencia sólida de efectos indirectos positivos: la contaminación también disminuye en las áreas cercanas a los límites de estas zonas. No obstante, estos efectos promedio esconden una gran heterogeneidad: las reducciones se concentran en las ciudades más grandes y densas, así como en aquellas con zonas de tamaño medio en relación con la superficie urbana total. Por el contrario, en las ciudades y zonas más pequeñas no se observa ningún efecto significativo.

Estos resultados sugieren que las LEZ generan beneficios ambientales a escala de toda la ciudad que van más allá de sus límites formales, lo que es coherente con la existencia de efectos de red y difusión tecnológica que superan los posibles efectos de desplazamiento.

Para contextualizar estos resultados, estimamos la elasticidad entre contaminación y densidad en ciudades europeas utilizando variables instrumentales basadas en patrones históricos de asentamiento. Encontramos que un aumento del 1 % en la densidad de población incrementa la exposición a las PM2.5 un 6 %, aproximadamente la mitad de lo observado en ciudades de Estados Unidos.

Interpretamos estos hallazgos mediante un modelo de equilibrio espacial que formaliza cómo las LEZ modifican la función de producción de contaminación en las ciudades monocéntricas. En conjunto, los resultados indican que las LEZ con niveles moderados de restricción, tal como se aplican habitualmente en Europa, generan reducciones agregadas de contaminación de aproximadamente el 1,8 % en el conjunto de la ciudad. En este proceso, predominan los efectos asociados al cambio modal del transporte y la renovación de la flota de vehículos, frente a los efectos del desplazamiento del tráfico.

Palabras clave: zonas de bajas emisiones, contaminación del aire, PM2.5, densidad urbana.

Códigos JEL: I10, Q53, Q58, R11, R12.

1 Introduction

Urban air pollution imposes substantial health and economic costs on European cities. The European Environment Agency estimates that in 2021 alone, at least 253,000 deaths in the European Union were attributable to fine particulate matter (PM2.5) concentrations exceeding the World Health Organization's recommended threshold of 5 $\mu g/m^3$ (European Environment Agency, 2023). Beyond mortality, pollution reduces labor productivity, increases healthcare expenditures, accelerates infrastructure deterioration, and depresses property values (Graff Zivin and Neidell, 2012; Hanna and Oliva, 2015; Anderson, 2019). In response to these costs and to meet European Green Deal targets —a 55% reduction in pollution-related premature deaths by 2030 relative to 2005 levels— municipal governments across Europe have increasingly adopted LEZs as a primary policy instrument to curb urban air pollution.

LEZs restrict the entry of high-emission vehicles, particularly older diesel cars, into designated urban areas. As of 2025, over 320 LEZs had been implemented across European cities, making this one of the continent's most widespread environmental policies. Yet despite their prevalence, rigorous empirical evidence on LEZ effectiveness remains surprisingly limited. Existing studies focus predominantly on individual cities —Madrid (Galdon-Sanchez et al., 2023), London (Leape, 2006), or German municipalities (Wolff, 2014)— yielding estimates that vary dramatically across contexts. Galdon-Sanchez et al. (2023), for instance, document a 19% reduction in PM2.5 within Madrid Central, while Bernardo et al. (2021) report more modest effects of 2-4% across a broader sample of European LEZs. This heterogeneity raises fundamental questions about the average effectiveness of LEZ policies across the European urban system and the mechanisms through which they operate.

A critical gap in the LEZ literature concerns *spatial spillovers*, i.e., the possibility that restricting emissions within a designated zone alters pollution levels in surrounding areas. Theoretical considerations suggest spillovers could be either positive or negative. On one hand, LEZs may displace traffic and polluting vehicles to peripheral routes, increasing pollution outside the restricted zone (a displacement effect). On the other hand, LEZs may generate city-wide benefits through network effects (reduced congestion on arterial roads), technology adoption spillovers (vehicle fleet upgrades extending beyond the LEZ boundary), and modal shift complementarities (improved public transport serving adjacent areas). Determining which channels dominate is essential for evaluating whether LEZs merely redistribute pollution spatially or achieve genuine city-wide reductions in exposure. Yet with few exceptions (Bernardo et al., 2021), existing studies do not explicitly estimate spillover effects, leaving this question unresolved.

This paper provides the first systematic continental-scale evaluation of LEZ effectiveness, focusing explicitly on both within-zone impacts and spatial spillovers. We construct a high-resolution geospatial panel dataset covering $1km x 1km$ grid cells across 33 European countries from 2007 to 2022, combining granular pollution measurements (PM2.5), ambient population data capturing 24-hour economic activity, and comprehensive LEZ implementation records obtained through web scraping and human annotations. Using a staggered difference-in-differences design that accounts for spatial spillovers (Butts, 2023), we estimate that LEZ adoption reduces population-weighted PM2.5 exposure by approximately 4% within designated zones. Crucially, we find robust evidence of *positive spillovers*: pollution also declines in areas adjacent to the LEZ boundary, and the pollution-distance gradient flattens throughout the city post-implementation. These findings suggest that LEZs generate city-wide environmental benefits that extend beyond their formal boundaries, consistent with network effects and technology spillovers dominating displacement mechanisms.

To contextualize our LEZ findings and understand the mechanisms through which density mediates policy effectiveness, we estimate the elasticity between urban population density and pollution exposure. This relationship is fundamental to evaluating LEZ impacts, as policies may induce household relocation and density adjustments that feed back into pollution levels. Using an instrumental variables strategy that exploits exogenous variation in historical settlement patterns —historical population density (Ciccone and Hall, 1993), soil quality (Combes et al., 2010), and aquifer presence (Burchfield et al., 2006)— we find that a 1% increase in population density is associated with a 6% increase in PM2.5 exposure in European cities. This elasticity is approximately half the magnitude documented for US cities by Carozzi and Roth (2023), who report an elasticity of 0.14 using comparable methods. The lower European elasticity suggests that differences in urban form, transport systems, or industrial structure moderate the pollution-density relationship, a pattern we return to when interpreting LEZ effectiveness.

Figure 1 illustrates the strong spatial correlation between population density and PM2.5 concentrations across Europe. The Figure reveals a positive relationship between experienced density —the average density within a 10km radius of each resident (Henderson et al., 2021; Duranton and Puga, 2020)—and population-weighted PM2.5 exposure across major European cities. This motivating fact underscores the importance of understanding how agglomeration economies, while generating productivity benefits, simultaneously impose environmental costs on urban residents. It also provides essential context for evaluating LEZ policies: to the extent that LEZs alter density distributions or commuting patterns, the pollution-density elasticity determines the magnitude of second-order effects on exposure.

Figure 1: Experienced Density vs. PM2.5

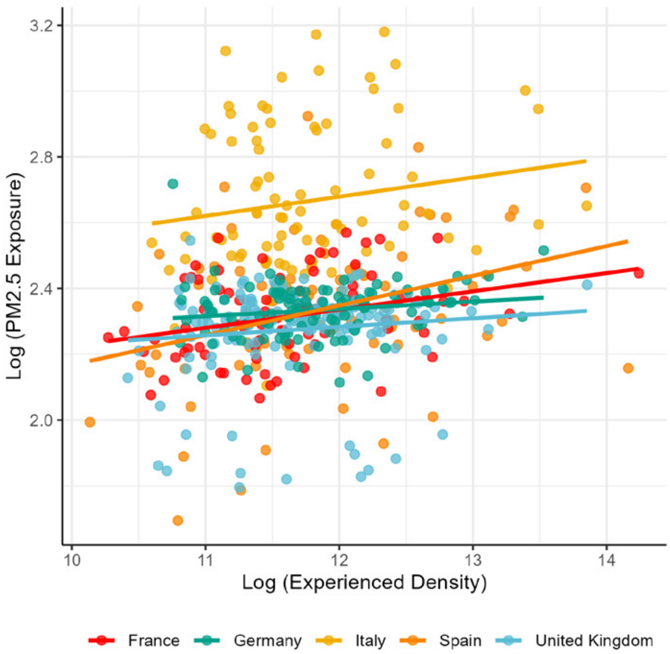

Notes: Data for 2019. The figure shows all cities in 2019 for the top 5 European countries by population. Experienced density is expressed in millions of persons. There is a positive correlation between experienced density and pollution exposure. For more info. about the data, please consult section 2.

Our estimate of a 4% reduction in within-zone pollution is substantially smaller than the 19% effect documented by Galdon-Sanchez et al. (2023) for Madrid Central but closely aligns with Bernardo et al. (2021), who report reductions of 2-4% across multiple European LEZs. This heterogeneity reflects important differences in policy design, enforcement stringency, and local context. Madrid Central represents an unusually aggressive intervention, banning nearly all non-resident vehicles from the city center with rigorous camera enforcement, in a city with high initial pollution levels and limited public transport alternatives at the time of implementation. By contrast, our sample includes LEZs with varying degrees of stringency, vehicle restrictions (e.g., diesel-only bans vs. comprehensive restrictions), and enforcement mechanisms. We interpret our 4% estimate as the *average treatment effect* of LEZ adoption across diverse European contexts, reflecting the typical policy implementation rather than the upper bound of what is achievable under ideal conditions.

Moreover, our analysis extends beyond Madrid Central's focus on within-zone effects to systematically quantify spillovers. While Galdon-Sanchez et al. (2023) document localized reductions, they do not examine whether pollution is displaced to adjacent neighborhoods or whether the policy generates city-wide benefits. Our finding of positive spillovers —pollution reductions extending beyond the LEZ boundary— suggests that even moderately-stringent LEZs can produce aggregate welfare gains through network effects and technology diffusion. This distinction between within-zone and city-wide effects is central to policy evaluation: a 4% within-zone reduction coupled with positive spillovers may generate greater aggregate benefits.

This paper makes four primary contributions. First, we provide the first systematic evaluation of LEZ effectiveness at a continental scale, estimating average treatment effects across a heterogeneous set of European cities while explicitly accounting for spatial spillovers. Methodologically, we extend the recent causal inference framework for settings with spatial spillovers (Butts, 2023) to the LEZ context, distinguishing between direct effects on treated areas and indirect effects on adjacent neighborhoods. Our finding that spillovers are negative, in the sense that LEZs reduce pollution beyond their formal boundaries, represents a novel empirical contribution to the LEZ literature and provides evidence that network effects and technology adoption dominate displacement mechanisms in practice.

Second, we contribute to the growing literature on the environmental costs of urban agglomeration. Building on Carozzi and Roth (2023)'s analysis of US cities, Borck and Schrauth (2022)'s global estimates, and Borck and Schrauth (2021)'s German results, we provide the first comprehensive estimates of the pollution-density elasticity for Europe using high-resolution spatial panel data. Our finding that European elasticities are approximately half those observed in the US raises important questions about the mechanisms through which urban form, transport systems, and industrial structure mediate environmental externalities. Moreover, by estimating this elasticity in the same spatial panel used to evaluate LEZs, we provide a direct link between the forces generating pollution (density) and the policies designed to mitigate it. This integration allows us to interpret LEZ effects through the lens of how policies alter the fundamental pollution production function in cities.

Third, we develop a spatial equilibrium model of a monocentric city that formalizes the mechanisms through which urban density and LEZs affect pollution exposure. Extending the canonical Alonso-Muth-Mills framework (Alonso, 1964; Mills, 1967) to incorporate a pollution production function in which pollution depends on both distance to the Central Business District (CBD), capturing commuting emissions and residential density, capturing congestion externalities, we derive testable predictions about LEZ impacts and spillover effects. The model clarifies the conditions under which LEZs generate negative versus positive spillovers and provides a theoretical foundation for interpreting our empirical findings. By linking reduced form estimates to structural parameters in the pollution production function, the model also guides future research on optimal LEZ design and spatial targeting.

Fourth, we introduce a novel high-resolution geospatial panel dataset that advances the empirical toolkit for studying urban environmental policies. Our dataset combines fine-scale pollution measurements ($1km$ grid cells), ambient population data from LandScan that captures true 24-hour economic activity rather than residential census counts, and comprehensive LEZ implementation records. The granularity and temporal coverage of this dataset, covering 15 years, 33 countries, and over 70 LEZs, enables identification of policy effects through within-city spatial and temporal variation, overcoming the challenges of confounding and selection that plague city-level analyses. We view this data infrastructure as a public good for future research on urban environmental policies in Europe.

Our paper builds on three strands of the urban environmental economics literature. First, we contribute to research evaluating the effectiveness of LEZs and related driving restrictions. Wolff (2014) document a 9% decrease in PM10 levels following LEZ implementation in Germany, while Bernardo et al. (2021) compare LEZs to urban tolls across European cities, reporting pollution reductions comparable to our estimates. Galdon-Sanchez et al. (2023) analyze Madrid Central using a sharp spatial regression discontinuity design, finding substantial localized reductions in both pollution (19%) and consumer spending (21%). Outside Europe, Blackman et al. (2018) study Mexico's driving restrictions, Blackman et al. (2020) examine Beijing's policies, and Leape (2006) evaluate London's congestion charge. Our contribution is to provide systematic evidence at a continental scale while explicitly quantifying spatial spillovers—a dimension largely absent from prior work despite its critical importance for welfare evaluation.

Second, we contribute to the literature estimating the elasticity between urban density and pollution exposure. Carozzi and Roth (2023) provide the most comparable framework, using instrumental variables and high-resolution spatial data to estimate elasticities for US cities. We adopt similar instruments, methodologies, and data structures, allowing direct comparison across continents. Our finding that European elasticities (0.06) are approximately half those in the US (0.14) aligns with Borck and Schrauth (2022), who document substantial cross-country heterogeneity in pollution-density relationships using coarser spatial units ($10km^2$) and single-year data. Borck and Schrauth (2021) report an elasticity of 0.08 for Germany based on ground monitoring data, closely matching our European average. Ahlfeldt and Pietrostefani (2019) synthesize estimates across countries, noting that elasticities are substantially higher in rapidly urbanizing contexts such as China. A natural extension of our work is to investigate the factors driving cross-continental differences in pollution-density elasticities, potentially linked to urban form, transport mode shares, or industrial composition.

Third, our spatial equilibrium model contributes to the theoretical literature on urban environmental externalities. Balboni and Shapiro (2025) emphasize the importance of evaluating localized environmental policies within broader urban spatial equilibrium models, noting that ignoring general equilibrium effects can lead to misleading welfare conclusions. Our model extends the Alonso-Muth-Mills framework by endogenizing pollution exposure as a function of both commuting (distance effects) and congestion (density effects), allowing us to characterize the spatial incidence of pollution costs and predict how LEZs alter equilibrium allocations. This framework complements recent quantitative spatial models in environmental economics while remaining tractable enough to yield clear analytical predictions. The model's key insight that spillover signs depend on whether network effects dominate displacement effects provides theoretical guidance for interpreting our empirical findings and designing future policies.

More broadly, our findings contribute to research on the costs and benefits of urban agglomeration. While agglomeration generates productivity gains (Duranton and Puga, 2020; Combes et al., 2011), it also imposes environmental costs through increased pollution exposure. The tension between these forces shapes optimal city size and the welfare effects of policies that alter urban form. Our estimates of both the pollution-density elasticity and LEZ effectiveness provide quantitative benchmarks for this tradeoff in the European context, complementing existing estimates for the US (Carozzi and Roth, 2023) and other regions. By linking these two sets of estimates—the costs of density and the effectiveness of policies to mitigate them—we provide a more complete picture of the environmental dimension of urban agglomeration externalities.

The remainder of this paper is structured as follows. Section2 provides institutional background on European air quality policy and LEZ implementation, describes our data sources and sample construction, and presents descriptive statistics. Section 3 outlines our empirical strategy, detailing the spatial difference-in-differences framework for estimating LEZ effects and the instrumental variables approach for identifying the pollution-density elasticity. Section 4 presents our main results on LEZ effectiveness, spatial spillovers, dynamic treatment effects, and heterogeneous impacts across city characteristics, followed by estimates of the pollution-density elasticity at both between-cities and within-cities scales. Section 5 conducts extensive robustness checks, examining sensitivity to sample composition, control group definitions, alternative estimators, and instrument validity. Section 6 develops a spatial equilibrium model of a monocentric city that formalizes the mechanisms through which density and LEZs affect pollution, derives testable predictions, and empirically validates the pollution production function. Section 7 concludes by discussing policy implications and directions for future research.

2 Background and Data

2.1 Institutional Background

European air quality policy is shaped by a multi-tiered regulatory framework combining supranational directives with local implementation. At the EU level, the 2008 Ambient Air Quality Directive (2008/50/EC) establishes binding limits for PM2.5 concentrations: an annual mean of 25 μg/m³ (later tightened to 20 μg/m³ in 2015) and a target value of 20 μg/m³ by 2020. Member states exceeding these thresholds face infringement proceedings and potential fines. The European Green Deal, launched in 2019, commits to further reductions, targeting a 55% decrease in pollution-related premature deaths by 2030 relative to 2005 levels and alignment with WHO guidelines (5 μg/m³) by 2050. These commitments create strong incentives for local authorities to adopt pollution-reduction measures, particularly in urban areas where concentrations are highest and population exposure is greatest.

LEZs have emerged as the primary local policy response. LEZs restrict vehicle access to designated areas based on emission standards, typically enforced through automated license plate recognition systems (e.g., London, Madrid) or periodic police checks (e.g., German cities). LEZ designs vary substantially across cities. Some target only diesel vehicles, while others impose broader restrictions including older gasoline vehicles or mandate minimum Euro emission standards (Euro 4 or higher in Milan and Rome, Euro 6 in Madrid Central). Enforcement stringency also varies: London's Ultra Low Emission Zone imposes daily charges of £12.50 for non-compliant vehicles, while many German LEZs rely on fines issued during spot checks, creating weaker incentives for compliance. These design differences affect both the magnitude of pollution reductions and the mechanisms through which they operate.

The institutional context also shapes the spatial incidence of LEZ effects. Most LEZs target historical city centers where employment and commercial activity are concentrated, closely corresponding to the CBD in standard urban models. However, city boundaries in our data are defined not by administrative jurisdictions but by functional urban areas (FUAs) based on population density and spatial contiguity (Duranton and Rosenthal, 2021). This distinction is critical: a LEZ covering Amsterdam's administrative center actually treats only the core of a much larger FUA extending into adjacent municipalities. This mismatch between policy boundaries and economic geography motivates our focus on within-city spatial variation, as it allows us to observe pollution changes both inside the LEZ, in spillover zones immediately adjacent to the boundary, and in untreated areas of the same functional city.

2.2 Data Sources and Sample Construction

Our empirical analysis draws on multiple data sources that we integrate into a spatially explicit panel dataset. The unit of observation varies by analysis: for the LEZ evaluation, we use $1km1km$ grid cells within cities over time; for the pollution-density elasticity, we construct both city-level aggregates (between-cities analysis) and grid-cell panels (within-cities analysis).

City Delineation. Defining cities using administrative boundaries introduces measurement error, as jurisdictional definitions often fail to align with the spatial extent of economic activity (Duranton and Rosenthal, 2021). We instead rely on the Global Human Settlement Settlement Model Layers (GHS-SMOD) from the European Commission's Joint Research Centre, which delineates urban centers based on gridded population and built-up area data (Commission and Eurostat, 2021). Specifically, grid cells are classified as urban centers if they (i) form a contiguous cluster with density exceeding 1,500 inhabitants per km^2 and (ii) contain at least 50,000 inhabitants within the cluster, with smoothed boundaries to avoid artificial discontinuities. This definition captures FUAs —regions where residents interact economically through commuting, shopping, and service provision, rather than administrative units.

Figure 2 illustrates this delineation for several major European cities. The green boundaries represent GHS-SMOD urban center definitions, while the color intensity reflects ambient population density (discussed below). Note that these boundaries often extend beyond administrative city limits (e.g., Greater London) or exclude sparsely populated areas formally within municipal jurisdictions. An example of the difference between the administrative delimitation and the one used by us can be seen in Figure 8 of the Appendix, where both delimitations are superimposed. Our analysis uses 2020 boundaries applied consistently across all years to avoid endogenous changes in city extents correlated with pollution or policy adoption. This yields a sample of 813 urban areas across 34 European countries, covering approximately $64,273km$ of urban land and $\tilde{1}10$ million residents (20% of the country sample population as of 2022).

Figure 2: European Urban Centers: Population Density and City Delineation

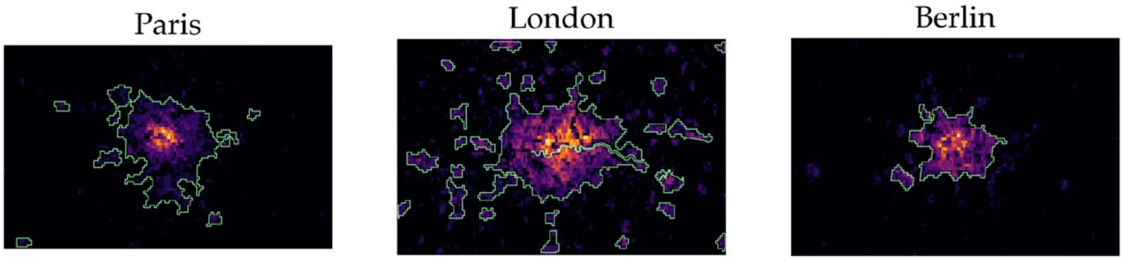

Notes: Ambient population density in 2021 from LandScan. Green boundaries delineate urban centers using GHS-SMOD classification (2020 boundaries applied to all years). Each pixel represents $1km^2$. These cities correspond to the regions displayed in of Figure 6 in the Appendix, where boundaries represent FUAs rather than administrative jurisdictions.

Pollution: PM2.5. Our pollution measure is fine particulate matter (PM2.5), i.e., inhalable particles with diameters smaller than 2.5 micrometers. PM2.5 comprises a mixture of nitrates, sulfates, ammonium, elemental carbon, and organic compounds, emitted directly from combustion sources (vehicles, power plants, industrial facilities) or formed through atmospheric chemical reactions involving sulfur dioxide and nitrogen oxides. We focus on PM2.5 rather than coarser particulates (PM10) or gaseous pollutants (NO_2, SO_2) because it is the most harmful to human health, penetrating deep into the respiratory system and entering the bloodstream. The WHO identifies PM2.5 as a leading environmental risk factor for mortality, with no safe threshold of exposure.

We obtain PM2.5 concentration data from the European Environment Agency's (EEA) gridded pollution dataset, which provides annual mean concentrations at $1km1km$ resolution across Europe from 2007 to 2022. The EEA constructs these grids using a regression-interpolation-merging methodology that combines: (i) ground monitoring data from approximately 3,500 air quality stations (the AirBase network), (ii) satellite-derived aerosol optical depth measurements (MODIS), (iii) chemical transport model outputs (EMEP), and (iv) land use covariates (road networks, emission inventories). The methodology first estimates a spatial regression model predicting pollution at monitoring locations as a function of satellite and land use data, then applies the fitted model to unmonitored locations, and finally merges predictions with observed values at monitoring stations using optimal interpolation. This approach balances the spatial coverage of satellite data with the accuracy of ground measurements.

For the between-cities analysis, we construct population-weighted PM2.5 exposure for city c in year t as:

$$Y_{ct} = \sum_{i=1}^{N_c} Y_{ict} \times \frac{Pop_{ict}}{Pop_{ct}} \tag{1}$$

where N_c is the number of $1km1km$ grid cells within city c, Y_{ict} is the PM2.5 concentration in cell i of city c in year t, and Pop_{ict} is the population of that cell. This weighting scheme reflects the exposure to pollution that residents actually experience rather than simple spatial averages, which would overweight unpopulated areas. For the within-cities analysis, the unit of observation is the grid cell, so we use Y_{ict} directly. In the LEZ analysis, we similarly use cell-level pollution.

Population Density and Economic Activity. We measure population density using the Oak Ridge National Laboratory's LandScan dataset, which provides annual estimates of *ambient population* —the average number of individuals present in each $1km1km$ grid cell over a 24-hour period (Sims et al., 2023). This is a critical distinction from traditional census data, which assign residential population to cells based on nighttime residence. Ambient population captures daytime economic activity, including commuting flows, workplace concentration, and commercial activity, making it a superior measure of the spatial distribution of economic activity relevant for pollution generation. LandScan constructs ambient population estimates using a dasymetric modeling approach that integrates: (i) nighttime lights satellite imagery (VIIRS), (ii) road network density (OpenStreetMap), (iii) land use classifications (Corine Land Cover in Europe), and (iv) census-based residential population (disaggregated to fine spatial scales using machine learning algorithms). The key advantage of ambient population over census-based measures is that it captures the agglomeration of economic activity that drives pollution generation. Consider a CBD with few residents but dense daytime employment: census data would show low population, while ambient population correctly identifies high economic activity and associated vehicle traffic, energy consumption, and emissions. This distinction is particularly important for evaluating LEZs, which target daytime activity (commuting, deliveries) rather than residential presence. Henderson et al. (2021) demonstrate that ambient population measures capture agglomeration economies more accurately than residential population, yielding stronger correlations with productivity and infrastructure outcomes.

We employ two density measures in our analysis. First, *grid-level density* (D_{ict}) is simply the ambient population in cell i at time t, which given the cell size corresponds to population per km². Second, we construct *experienced density* following Roca and Puga (2017) and Henderson et al. (2021), defined as the population-weighted average density within a 10km radius of each resident:

$$D_{ict}^{\exp} = \sum_{j \in B_{10}(i)} D_{jct} \times \frac{Pop_{jct}}{Pop_{B_{10}(i)ct}} \quad (2)$$

where $B_{10}(i)$ denotes the set of cells within 10km of cell i. Experienced density better captures agglomeration effects by reflecting the density actually encountered by residents in their daily activities (commuting, shopping, accessing services), whereas grid-level density can be misleading when cities have heterogeneous spatial structures. We present results using both measures, with experienced density as our preferred one for the pollution-density elasticity analysis.

Low Emission Zones. We construct a comprehensive dataset of LEZ implementations in Europe through a combination of web scraping and manual verification. Our primary data source is the Urban Access Regulations project,[1] which documents LEZ policies across European municipalities, including implementation dates, vehicle restrictions, and geographic boundaries. We supplement this with municipal government websites, transport authority databases, and press releases to verify implementation dates and resolve ambiguities. In total, we identify 75 LEZ implementations across 65 cities in 11 countries between 2007 and 2022, with Germany accounting for the largest share (42 LEZs), followed by Italy (10 LEZs), France (7 LEZs), and United Kingdom (5 LEZs).

A critical component of our dataset is the spatial delineation of LEZ boundaries. For each LEZ, we downloaded the geospatial delineation from official municipal websites, mapping them to $1km1km$ grid cells that align with our pollution and population data. This allows us to classify each grid cell within a city as: (i) *treated* if located within an

[1] Available at https://urbanaccessregulations.eu/

LEZ boundary, (ii) *spillover* if located in a buffer zone adjacent to the LEZ, or (iii) *control* if located at a 5-10km distance from the LEZ border. We define two spillover zones to test the spatial decay of LEZ effects: 0-1km from the boundary (adjacent cells) and 1-3km from the boundary.

Figure 3: LEZ Treatment and Spillover Zones: London

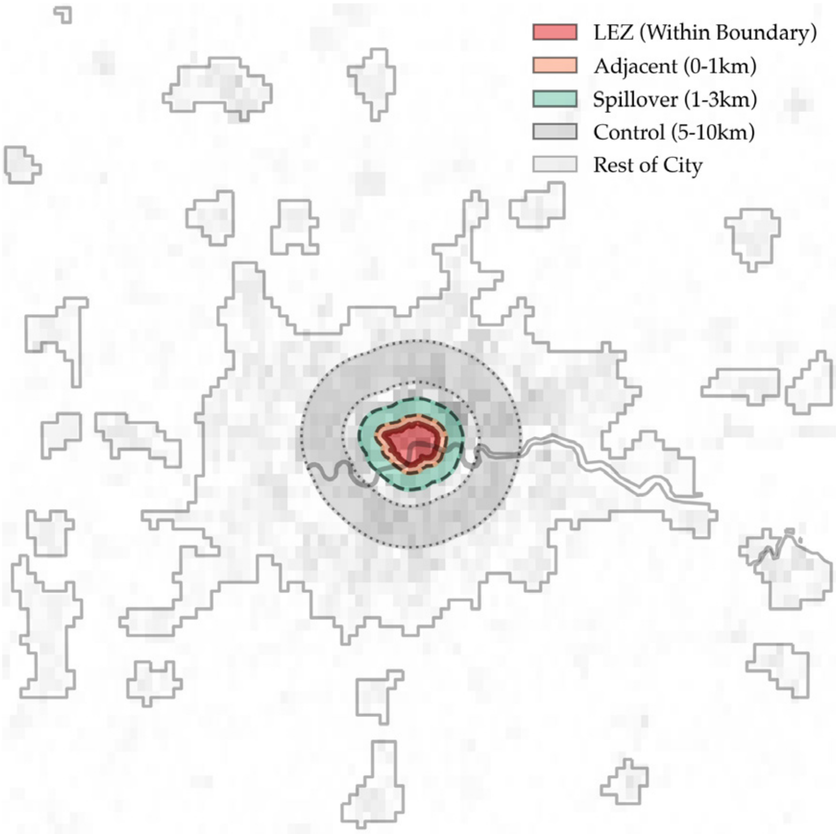

Notes: Ambient population in 2020 (LandScan). The red shaded area represents the LEZ boundary (treatment zone). Concentric buffers define the adjacent zone (0-1km, orange), spillover zone (1-3km, teal), and control zone (5-10km, gray). The light gray areas constitute the rest of the city outside our analytical sample. The control zone provides the counterfactual pollution trajectory under the parallel trends assumption.

Figure 3 illustrates our spatial treatment assignment using London's LEZ as an example. Each $1km1km$ grid cell is classified into one of four analytical zones based on its distance from the LEZ boundary: the LEZ zone itself (within boundary), the adjacent zone (0-1km buffer), the spillover zone (1-3km buffer), and the control zone (5-10km buffer). This zonification allows us to estimate not only the direct effect of LEZ policies on pollution within treated areas, but also potential spillover effects —either positive (pollution reduction through network effects and technology diffusion) or negative (pollution displacement through traffic diversion)— on neighboring untreated areas. The control zone, located sufficiently far from the LEZ boundary to avoid contamination while remaining within the same city, provides the counterfactual pollution trajectory under the parallel trends assumption. Cells beyond 10km from any LEZ boundary are excluded from the analysis to maintain sample homogeneity, though we test robustness to alternative control group definitions in Section 5.

Our LEZ sample exhibits staggered adoption, with implementation dates ranging from 2007 to 2022. This temporal variation is essential for identification, as it allows us to compare cities before and after LEZ adoption while controlling for common time trends. However, staggered adoption also creates challenges for estimation, as treatment timing may be correlated with unobserved city characteristics (e.g., pollution severity, political preferences, fiscal capacity). We address these concerns using recent difference-in-differences estimators designed for staggered settings and present extensive robustness checks, including event study specifications that test for pre-trends and dynamic treatment effects. Figure 4 displays the distribution of treated cells by country and relative time to LEZ implementation. The concentration of observations within ±8 years of implementation reflects our focus on medium-run effects and the recent proliferation of LEZs.

Figure 4: Treated Grid Cells by Country and Time Relative to LEZ Implementation

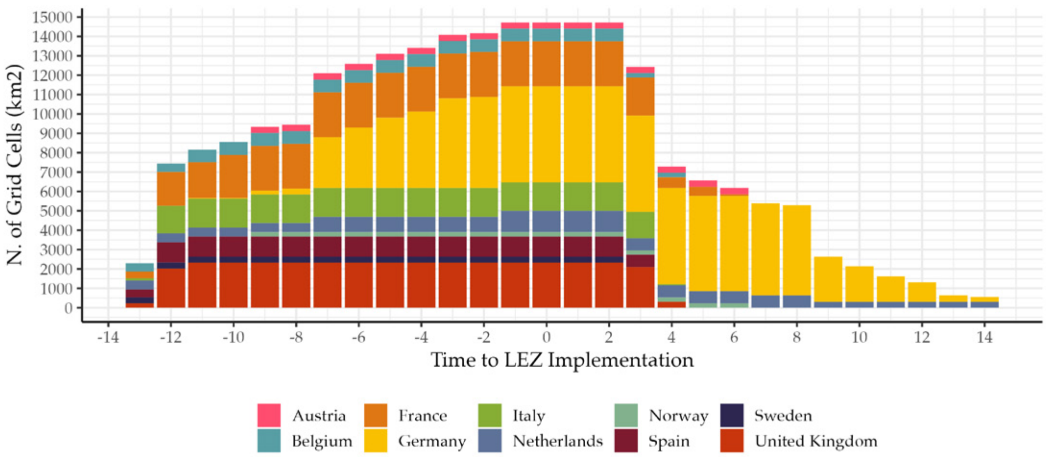

Notes: Distribution of treated 1km² grid cells by country across event time (years relative to LEZ implementation). Only cities with at least one LEZ are included. Germany dominates the sample due to widespread LEZ adoption (33 cities, 42 zones). The concentration of observations within ±8 years reflects our estimation window and recent LEZ proliferation.

A methodological complication arises in cities with multiple LEZs. Three large urban regions —North Rhine-Westphalia (8 LEZs across multiple municipalities), Düsseldorf and Dortmund (2 LEZs each), and Rotterdam-The Hague (2 LEZs)— contain overlapping or adjacent LEZ boundaries. Figure 10 in the Appendix illustrates this interference problem using the Rotterdam-The Hague metropolitan area, where two LEZs operate within 15km of each other. The overlapping buffer zones create an ambiguous treatment assignment: cells located 5-10km from Rotterdam's LEZ boundary (our intended control group) simultaneously fall within 1-3km of The Hague's LEZ boundary (the spillover zone). This spatial contamination violates the Stable Unit Treatment Value Assumption (SUTVA), as the control group for one LEZ receives spillover treatment from the other. We further exclude cities where the control zone (5-10km buffer) covers less than 10% of total city area, ensuring sufficient spatial variation for reliable counterfactual estimation. After cleaning our sample, these exclusions reduce the sample to 20 cities with their respective 20 LEZs.

2.3 Instrumental Variables for Population Density

Our identification of the pollution-density elasticity relies on three sets of instruments that isolate exogenous variation in population density uncorrelated with contemporary determinants of pollution. The instrumental variables approach addresses three sources of endogeneity: (i) omitted variables that affect both density and pollution (e.g., amenities, sectoral composition), (ii) reverse causality from pollution affecting location choices (Heblich et al., 2021), and (iii) measurement error in density arising from the uneven spatial distribution of economic activity. The instruments must satisfy relevance (strong first-stage correlation with density) and exclusion (affecting pollution only through density, not directly).

Historical Population Density. Following Ciccone and Hall (1993) and Carozzi and Roth (2023), we instrument contemporary density using historical population distributions —specifically, population density in 1800 CE. The identifying assumption is path dependence: settlements established in pre-industrial times for reasons unrelated to contemporary pollution (e.g., proximity to arable land, navigable rivers, defensive positions) persist as population centers today, but historical pollution sources differ fundamentally from modern ones. In 1800 CE, European pollution was dominated by wood burning and animal-powered transport, bearing little correlation with 21st-century vehicular emissions and industrial activity. We obtain historical population data from the History Database of the Global Environment (HYDE), which provides gridded population estimates from 10,000 BCE to 2015 CE at approximately 5km resolution (Goldewijk, 2017; Klein Goldewijk et al., 2017). We spatially interpolate these estimates to $1km1km$ cells to match our pollution and contemporary density data. The first-stage correlation between historical and contemporary density is strong —F-statistics exceed 500 in most specifications— reflecting the remarkable persistence of European settlement patterns over two centuries. Robustness checks using alternative historical lags (1500, 1000, 100 CE) yield nearly identical results, supporting the validity of the exclusion restriction.

Soil Quality. Our second instrument exploits variation in agricultural land quality, following Combes et al. (2010). High-quality soils historically attracted agricultural settlements, leading to persistent population concentrations even as economies transitioned from agriculture to industry and services. We use data from the Harmonized World Soil Database (HWSD), which classifies soils into seven quality categories based on constraints for agricultural use: no constraints, slight constraints, moderate constraints, severe constraints, very severe constraints, unsuitable and non-soil (water, rock) (IIASA, 2023). Constraints are assessed in six dimensions: nutrient availability and retention, rooting conditions, oxygen availability, excess salts, toxicity, and workability. We construct a soil quality index as the share of land in each grid cell (or city) classified as having no or slight constraints for agriculture. This index strongly predicts contemporary density—fertile areas like the Po Valley, the Rhine corridor, and East Anglian plains remain densely populated— but plausibly satisfies the exclusion restriction: subsurface soil characteristics do not directly affect PM2.5 concentrations except through their influence on population distribution. We cannot entirely rule out indirect channels (e.g., soil quality affecting agricultural burning practices, dust emissions from tilled land), but these are likely negligible in urban areas where agriculture has ceased.

Aquifer Presence. Our third instrument follows Burchfield et al. (2006), using the presence and productivity of groundwater aquifers. Aquifers reduce the cost of urban development by providing readily accessible water for residential and industrial use, encouraging population concentration. We classify aquifers into four productivity categories: highly productive porous aquifers, moderately productive aquifers, low-productivity aquifers, and non-aquifer regions (bedrock or impermeable formations). Data come from the European Aquifer Database, compiled by the International Groundwater Resources

Assessment Centre (IGRAC) (Duscher and Günther, 2019). The exclusion restriction requires that aquifers affect pollution not directly but only through population density. This is plausible in contemporary settings where water supply networks are ubiquitous: while aquifers historically determined settlement feasibility, modern cities obtain water from diverse sources (surface reservoirs, inter-regional transfers, desalination), severing the direct link between subsurface water and pollution.

Table 12 presents descriptive statistics for all three instruments. Historical population density exhibits substantial variation, with a mean of 1.47 million inhabitants per city in 1800, reflecting the concentration of population in cities.

2.4 Control Variables

Our specifications include a rich set of controls to address omitted variable bias and improve precision. These fall into four categories: climatic, geographic, trade-related, and pollution-source controls.

Climate Variables. We control for temperature, precipitation, and wind speed, all of which affect PM2.5 concentrations through dispersion and chemical formation mechanisms. Data come from the E-OBS gridded climate dataset, which provides daily observations at 0.1° resolution (approximately 10km) covering Europe from 1950 to present (Cornes et al., 2018). We aggregate daily observations to annual means for temperature and wind speed, and annual totals for precipitation, then spatially match these to our $1km1km$ grid cells. Temperature affects pollution through multiple channels: higher temperatures accelerate photochemical reactions that form secondary PM2.5, but also increase atmospheric mixing that disperses pollutants. Precipitation removes airborne particles through wet deposition (rain and snow), yielding a negative correlation between precipitation and PM2.5. Wind speed improves dispersion, reducing local concentrations. Controlling for these variables is critical to isolating the effect of density from mechanical pollution dispersion driven by weather.

Geographic Controls. We control for latitude, terrain ruggedness, elevation, coastal proximity, and distance to major rivers. Latitude proxies for solar radiation and temperature gradients. Terrain ruggedness —the average elevation difference between each cell and its neighbors, computed following Nunn and Puga (2012)— captures topographic constraints on pollution dispersion. Valleys and basins trap pollutants (e.g., the Po Valley, the Balkan regions), while elevated areas experience cleaner air. Coastal proximity affects climate (moderating temperatures, increasing wind speeds) and potentially pollution through maritime emissions and sea-breeze circulation patterns. We define a city as coastal if its centroid is within 50km of the nearest coast. Geographic data come from Natural Earth Data (coastlines, rivers) and the European Environment Agency (elevation and derived terrain ruggedness).[2] These controls are time-invariant, so they are absorbed by cell or city fixed effects in panel specifications.

Trade-Related Controls. Following Carozzi and Roth (2023), we control for coastal location and proximity to navigable waterways to address potential confounding from port activities and trade exposure. Coastal cities may have higher pollution from shipping emissions, but also different industrial structures (less heavy manufacturing, more services) and transport mode shares (more maritime freight, less trucking), complicating the interpretation of the density coefficient. Controlling for trade access reduces this bias.

Pollution Source Controls. We control for proximity to major stationary pollution sources —specifically, coal, oil, and gas power plants. Data come from the Global Power Plant Database, which geocodes 35,000 power plants worldwide with information on fuel type, capacity, and (when available) annual generation (Global Energy Observatory, 2018). For each grid cell or city, we compute the distance to the nearest pollutant-emitting power plant (coal, oil, or gas). Power plants are major point sources of PM2.5 precursors (SO_2, NO_x) and can confound the density-pollution relationship if located near urban centers.

2.5 Descriptive Statistics

Table 1 examines how pollution, density, and covariates vary across spatial zones during the post-implementation period in the 20 LEZ-adopting cities. We classify each grid cell into four mutually exclusive zones based on distance to LEZ boundaries: (i) LEZ zone (within the LEZ boundary), (ii) Adjacent zone (0-1km from the boundary), (iii) Spillover zone (1-3km from the boundary), and (iv) Control zone (5-10km from the boundary). These descriptives reveal spatial gradients in pollution and density that motivate our

[2] EEA Digital Elevation Model.

spillover analysis and inform our choice of control groups. Cells within LEZ boundaries exhibit the highest average pollution and density in the post-implementation period. Log PM2.5 is 2.63 (equivalent to 13.9 µg/m³), while log density is 7.65 (corresponding to approximately 2,096 persons per km²). This pattern reflects the fact that LEZs are typically implemented in city centers where both pollution exposure and population concentration are highest. Temperature averages 8.12°C, relatively warm compared to adjacent zones, potentially reflecting the urban heat island effect which is strongest in dense city centers with extensive impervious surfaces and concentrated heat-generating activities. Wind speed is 38.03 m/s × 100, notably higher than other zones, likely reflecting the channeling effects of narrow streets and tall buildings in dense urban cores where canyon effects accelerate wind flows at ground level. The LEZ zone is located relatively close to coasts (9,740 meters average, or 9.7 km) and very close to rivers (1,039 meters, or 1.0 km), consistent with the historical pattern of European cities developing along interior waterways where early urban centers established themselves for transportation, commerce, and water access.

Table 1: Descriptive Statistics by Spatial Zone (Post-Implementation Period)

Zone	Log $PM_{2.5}$	Log Dens.	Temp. (°C)	Precipitation (mm/day)	Wind (m/s)	Coast Dist. (km)	River Dist. (km)
LEZ	2.63	7.65	8.12	0.24	38.03	0.97	10.3
Adjacent (0-1km)	2.60	7.61	7.75	0.25	3.45	1.3	1.27
Spillover (1-3km)	2.56	7.44	7.66	0.26	3.45	1.01	1.16
Control (5-10km)	2.54	6.98	8.04	0.25	3.44	1.13	1.32

Notes: This table presents descriptive statistics by spatial zone during the post-implementation period for the 20 LEZ-adopting cities after cleaning our sample. Grid cells are classified into four mutually exclusive zones based on distance to LEZ boundaries: LEZ Zone (within boundary), Adjacent Zone (0-1km from boundary), Spillover Zone (1-3km from boundary), and Control Zone (5-10km from boundary). Log $PM_{2.5}$ represents natural logarithm of particulate matter concentration. Log Density represents natural logarithm of population per km². Temperature measured in degrees Celsius. Precipitation measured in millimeters per day. Wind speed reported in units of m/s × 100. Coast and river distances measured in kilometers. Sample restricted to cell-year observations within LEZ-adopting cities.

Cells immediately adjacent to LEZ boundaries (0-1km buffer) exhibit pollution and density levels nearly identical to the LEZ zone itself. Log PM2.5 is 2.60 (13.5 µg/m³) and log density is 7.61 (2,014 persons per km²), both only marginally lower than within the boundary but substantially higher than more distant zones. This similarity is expected: the 0-1km buffer captures neighborhoods contiguous to the LEZ—often indistinguishable from LEZ areas in terms of urban form, traffic patterns, and economic activity. The adjacent zone serves a critical role in our spillover analysis: if LEZ policies generate negative externalities through traffic displacement or residential relocation, pollution should increase in this zone relative to counterfactual trends; conversely, if positive spillovers dominate through network effects or technology adoption, pollution should decline. Temperature is cooler in the adjacent zone (7.75°C versus 8.12°C in LEZ areas), potentially reflecting reduced urban heat island intensity as building density decreases and green space increases moving away from the dense core. Wind speed drops to 34.55 m/s × 100, more typical of urban areas without the extreme channeling effects of the densest zones. The adjacent zone is located farther from coasts (10,383 meters or 10.4 km) and rivers (1,278 meters or 1.3 km) compared to LEZ zones, reflecting the spatial expansion of cities outward from their waterway origins.

Cells in the Spillover zone (1-3km buffer) exhibit further declines in pollution and density, with log PM2.5 at 2.56 (12.9 μg/m^3) and log density at 7.44 (1,698 persons per km^2). This zone represents the transition from dense urban core to suburban neighborhoods, experiencing indirect LEZ effects through changes in through-traffic, modal shifts in public transport networks, and technology spillovers as vehicle fleets upgrade city-wide. Cells in the Control zone (5-10km from LEZ boundaries) serve as our primary comparison group, exhibiting notably lower pollution and density: log PM2.5 is 2.54 (12.7 μg/m^3), approximately 7% lower than the LEZ zone, while log density is 6.98 (1,074 persons per km^2), less than half the density of LEZ areas. These cells represent the urban periphery—areas sufficiently distant from the LEZ to be plausibly unaffected by direct policy spillovers. Lower pollution reflects both lower traffic intensity and better dispersion conditions.

Several key patterns emerge from the comparison of the four zones. First, there is a clear pollution-density gradient: moving from control zones (log PM2.5= 2.54, log density = 6.98) to LEZ zones (2.63, 7.65) represents a 9.5% increase in density and 3.5% increase in pollution. Second, the pollution gradient is relatively flat across zones (ranging only from 2.54 to 2.63), while density varies substantially (6.98 to 7.65), suggesting that factors beyond density —such as wind patterns, building configurations, and traffic composition— play important roles in pollution exposure. Third, climate variables show modest spatial heterogeneity: temperature varies non-monotonically across zones (7.66-8.12°C), wind speed is highest in LEZ zones (38.03 m/s × 100), validating the importance of controlling for weather in our specifications. Fourth, the geographic gradient reveals the European urban structure: LEZ zones are closest to rivers (1.0 km) and coasts (9.7 km), with distances increasing toward control zones (1.3 km, 11.3 km), reflecting historical development patterns where cities established cores along waterways and expanded outward.

Table 2 presents descriptive statistics for our main variables at two levels of aggregation: city-level averages (columns 1-2) and grid-cell observations (columns 3-4). The between-cities sample comprises 813 functional urban areas across 33 European countries observed annually from 2007 to 2022, yielding approximately 12195 city-year observations.

Table 2: Descriptive Statistics of Cities characteristics (Between and Within)

	Cities		Cells (1km2)	
	Mean	Std. Dev.	Mean	Std. Dev.
Density	0.13	0.34	0.16	0.66
Experienced Density	0.15	0.15	—	—
Pollution Exposure / PM2.5	14.63	5.68	12.12	4.83
Temperature	8.14	3.52	7.39	3.37
Precipitation	3.64	1.23	2.54	1.31
Wind Speed	2.59	1.29	3.33	1.12
Ruggedness	15.19	15.01	16.45	18.54
Coast City	0.46	0.50	—	—
Water Distance	128.10	146.93	2.09	1.70
Coast Distance	41.07	46.88	10.55	9.85
Power Plant Distance	563.77	387.66	97.17	296.19

Notes: Yearly (2007-2022) averages and standard deviation. "Cities" indicates that the unit of observation is the entire city, while "Cells" indicates that the unit of observation is a 1km² cell within cities. Population and experienced density is expressed in millions of persons, pollution is PM2.5, temperature in Celsius degrees, precipitation in milimiters per day, wind speed in meters per second (in thousands) at a 10 meter height above the surface, and all distance variables are expressed in kilometers (km). Water and coast distance is euclidean distance when comparing cells.

The average population density is 0.13 million people per km² at the city level and 0.16 per km² at the cell level. The larger cell-level variance reflects the steep density gradients within cities: central areas exhibit densities exceeding 10,000 persons per km², while peripheral cells are sparsely populated. We also report experienced density —the population-weighted average density within a 10km radius— which averages 0.15 million per km² at the city level. This measure better captures the concentration of economic activity that residents encounter in their daily lives and will serve as our preferred density measure in the IV analysis (Section 3). Population-weighted PM2.5 exposure averages 14.63 μg/m³ at the city level and 12.12 μg/m³ at the cell level. The lower cell-level mean reflects the fact that many peripheral cells have low population weights, pulling down the unweighted average. Both levels exhibit substantial cross-sectional variation. This variation motivates our focus on the pollution-density relationship: denser cities and denser neighborhoods within cities tend to have higher pollution exposure, but the magnitude of this elasticity remains an empirical question.

Climate variables —temperature, precipitation, and wind speed— exhibit expected geographic patterns. Average temperature is 8.14°C at the city level and 7.39°C at the cell level and wind speed averages 2.59 m/s (cities) and 3.33 m/s (cells). These climate variables play dual roles in our analysis: they affect pollution dispersion (wind removes particles, rain washes them out, temperature inversions trap them) and they correlate with settlement patterns (people prefer temperate climates, avoiding extremes), necessitating their inclusion as controls in both DiD and IV specifications. Geographic controls include terrain ruggedness (average 15.19 at city level, 16.45 at cell level), proximity to water bodies (coast distance averages 41.07 km for cities, 10.55 km for cells; river distance 128.10 km and 2.09 km respectively), and power plant proximity (563.77 km for cities, 97.17 km for cells). Power plant distance serves as a proxy for industrial pollution sources; the closer proximity at the cell level suggests that industrial facilities tend to be located in urban peripheries or adjacent to cities rather than in dense centers.

Tables 12 and 13 present descriptive statistics for the three instruments used to address endogeneity in the pollution-density relationship: historical population density, aquifer presence, and soil quality. These instruments exploit variation in settlement patterns determined by geographic and historical factors plausibly uncorrelated with contemporary pollution sources. Historical population density (Table 12, rows 1-4) captures the persistence of European urban settlements over millennia. Average population in 100 CE was 0.10 million per city, increasing to 0.13 million in 1000 CE, 0.43 million in 1500 CE, and 1.47 million in 1800 CE. The large standard deviations reflect extreme heterogeneity: Rome and Athens were major population centers in 100 CE (¿100,000 residents), while many Northern European cities did not yet exist. By 1800 CE, most contemporary cities were established, with populations ranging from a few thousand to over one million (London, Paris). We use 1800 CE population as our baseline instrument because: (i) it predates modern pollution sources (automobiles, coal-fired power plants) by a century, satisfying the exclusion restriction, and (ii) it exhibits the strongest correlation with contemporary density, providing instrument relevance. The earlier lags (100 CE, 1000 CE, 1500 CE) serve as robustness checks in Section 5.

For aquifer presence (rows 5-10), this instrument exploits variation in groundwater availability that historically determined settlement viability. We classify aquifers into six categories based on productivity (highly, low-to-moderately, locally, practically non-aquiferous) and type (porous, fissured). On average, 31% of city land overlays highly productive porous aquifers, 22% overlays low-to-moderately productive porous aquifers, and smaller shares have fissured or non-aquiferous bedrock.

Soil quality (Table 13) measures agricultural suitability across seven dimensions: excess salts, nutrient availability, nutrient retention, oxygen availability, rooting conditions, toxicity, and workability. We classify land into five quality levels: mainly non-soil (2-3% of land across dimensions), moderate limitations (21-24%), no or slight limitations (48-57%), severe limitations (9-13%), and very severe limitations (4-7%). On average, approximately half of city land has no or slight agricultural constraints, suitable for productive farming. The cross-dimensional variation allows us to test the robustness of our IV estimates to alternative soil-based instruments in Section 5.

3 Empirical Strategy

This section outlines the econometric strategies used to estimate: (i) the causal effect of LEZs on pollution exposure, accounting for spatial spillovers, and (ii) the elasticity between population density and pollution exposure. The LEZ analysis is our primary contribution and receives extended treatment. We present the difference-in-differences framework first, then turn to the instrumental variables (IV) approach for the density elasticity, which provides essential context for interpreting LEZ mechanisms.

3.1 LEZ Effectiveness: Difference-in-Differences with Spatial Spillovers

Estimating the causal effect of LEZs on pollution requires addressing two fundamental identification challenges. First, LEZ adoption is endogenous: cities implementing LEZs differ systematically from non-adopters in observable characteristics (size, density, baseline pollution levels, political preferences) and likely in unobservables (environmental preferences, administrative capacity, fiscal resources). Simply comparing pollution levels between adopters and non-adopters would confound policy effects with these pre-existing differences. Second, LEZs generate spatial spillovers —changes in pollution outside the designated zone induced by the policy. Ignoring spillovers violates the SUTVA, potentially biasing estimates of both within-zone effects and the net impact on city-wide exposure. We address the first challenge using a difference-in-differences (DiD) design that exploits the staggered rollout of LEZs across European cities from 2007 to 2022. By comparing changes in pollution within treated areas (inside LEZ boundaries) to changes in control areas (untreated neighborhoods within the same city) over the same period, we difference out time-invariant unobservables and control for common time trends. The identifying assumption is parallel trends: absent the LEZ, treated and control areas would have experienced the same pollution trajectory. We address the second challenge by adopting the framework of Butts (2023), which extends standard DiD to settings with spatial spillovers. Rather than defining a binary treatment indicator, we partition space into three zones: (i) *treated* cells located within LEZ boundaries, (ii) *spillover* cells located in buffers adjacent to LEZ boundaries (where indirect effects may occur), and (iii) *control* cells located sufficiently far from LEZ boundaries to be unaffected.

The estimand of interest is not a single treatment effect but a vector of effects: the direct effect on treated cells, the indirect effect on spillover cells, and (by construction) a zero effect on control cells. Formally, let $Y_{ict}(T_{ict}, S_{ict})$ denote potential pollution in cell i of city c in year t as a function of own treatment status $T_{ict} \in \{0, 1\}$ and spillover exposure S_{ict}, defined as the share of cells within a specified radius (e.g., 3km) that are treated. The average treatment effect on the treated (ATT) is:

$$\text{ATT} = \mathbb{E}[Y_{ict}(1, S_{ict}) - Y_{ict}(0, S_{ict}) \mid T_{ict} = 1] \tag{3}$$

The spillover effect on untreated cells is:

$$\text{Spillover} = \mathbb{E}[Y_{ict}(0, S_{ict}) - Y_{ict}(0, 0) \mid T_{ict} = 0, S_{ict} > 0] \tag{4}$$

Standard DiD estimates a single parameter conflating these two effects. Our approach separately identifies them by leveraging spatial variation in distance to LEZ boundaries. We classify each $1km1km$ grid cell within LEZ-adopting cities into one of four categories based on its spatial relationship to the LEZ boundary:

1. **Treated (LEZ)**: Cells located within the LEZ boundary in years after implementation. For city c implementing an LEZ at time T_c^*, cell i is treated if $i \in \text{LEZ}_c$ and $t \geq T_c^*$.

2. **Spillover Zone 1 (0-1km)**: Cells located within 1km of the LEZ boundary but outside it. This zone captures immediate adjacent effects —commuters parking just outside the LEZ, traffic diverted to perimeter roads, or technology adoption by nearby residents.

3. **Spillover Zone 2 (1-3km)**: Cells located 1-3km from the LEZ boundary. This zone captures medium-range spillovers —changes in arterial road traffic, modal shifts extending beyond the immediate perimeter, or residential relocation induced by the policy.

4. **Control**: Cells located between 5 and 10km from any LEZ boundary. These cells serve as the counterfactual: areas within the same city (sharing the same labor market, political context, and time trends) but sufficiently distant from the LEZ to be unaffected by direct or spillover effects.

The choice of buffer distances reflects a tradeoff between spatial resolution and power. Narrower buffers (e.g., 0-500m) provide finer identification of spillover gradients but reduce sample size in each zone, inflating standard errors. Wider buffers increase power but may aggregate heterogeneous effects across different distances. Our 1km buffers balance these concerns and align with typical commuting distances in European cities. Figure 3 illustrates this classification for London. The control group comprises cells in the outer London urban area.

Thus, our baseline specification estimates separate treatment effects for each zone using a two-way fixed effects (TWFE) regression:

$$\ln(Y_{ict}) = \beta^{\text{LEZ}} \cdot \text{LEZ}_{ict} + \sum_{k=1}^{3} \beta^k \cdot \text{Spillover}_{ict}^k + \gamma' X_{ict} + \alpha_{ic} + \delta_t + \epsilon_{ict} \tag{5}$$

where Y_{ict} is population-weighted PM2.5 concentration in cell i, city c, year t (in µg/m³), LEZ_{ict} is an indicator equal to 1 if cell i is within an LEZ boundary in year $t \geq T_c^*$,

Spillover^k_{ict} are indicators for spillover zones $k \in \{1, 2, 3\}$ in post-treatment years, X_{ict} is a vector of time-varying controls (temperature, precipitation, wind speed), α_{ic} are cell fixed effects, absorbing time-invariant unobservables (baseline pollution, geography), δ_t are year fixed effects, absorbing aggregate trends (EU regulations, economic cycles, vehicle fleet evolution) and ϵ_{ict} is an idiosyncratic error term, clustered at the city level to allow arbitrary correlation within cities over time. The parameter β^{LEZ} identifies the average treatment effect on treated cells, interpreted as the causal effect of LEZ implementation on pollution within the designated zone. The parameters $\{\beta^1, \beta^2, \beta^3\}$ identify spillover effects at different distances. If spillovers are negative (network effects and technology adoption dominate), we expect $\beta^k < 0$ and potentially $|\beta^1| > |\beta^2| > |\beta^3|$ (spatial decay). If spillovers are positive (displacement dominates), we expect $\beta^k > 0$. The null hypothesis of no spillovers corresponds to $\beta^1 = \beta^2 = \beta^3 = 0$.

We log-transform pollution concentrations for three reasons. First, the distribution of PM2.5 is right-skewed, and log transformation reduces the influence of outliers. Second, coefficients are interpretable as semi-elasticities. Third, treatment effects are more likely to be proportional rather than additive: a 1 µg/m³ reduction is more meaningful in a low-pollution city than a high-pollution city . We include time-varying climate controls (X_{ict}) because weather affects both pollution dispersion and commuting behavior. Temperature inversions trap pollutants near the surface, precipitation removes particles via wet deposition, and wind speed enhances dispersion. These variables exhibit seasonal and interannual variation uncorrelated with LEZ adoption (conditional on fixed effects), so they are plausibly exogenous. We do not control for time-varying economic variables (employment, GDP) because these are potential mechanisms through which LEZs affect pollution (e.g., LEZs may reduce commercial activity in treated zones, lowering traffic). Including them would constitute "bad controls" that absorb treatment effects we aim to estimate.

Control Group Construction and Identification Assumptions. The validity of equation (5) hinges on the parallel trends assumption: absent treatment, treated and control cells would have experienced identical pollution trends. As a descriptive prelude to the formal event study, Appendix Figure 9 plots average log PM2.5 across the four spatial zones against years relative to LEZ implementation. Because these are raw zone means (with no fixed effects or controls), all four zones share the broad secular decline in European PM2.5 driven by tightening EU emission standards and fleet turnover. The figure is therefore informative about pre-period co-movement across zones, not about the treatment effect itself, which we isolate net of common trends in the event study below (Figure 5).

The figure reveals three key patterns. First, the pre-treatment period (years -12 to 0) exhibits remarkably parallel trends across all four zones. All lines track closely together, declining gradually from approximately 2.80 in year -12 to 2.50-2.55 in year 0. The parallelism is particularly tight from year -8 onward, with no systematic divergence between treated (LEZ, Adjacent, Spillover) and control areas. This visual evidence supports the parallel trends assumption: absent LEZ adoption, pollution trajectories would have remained parallel. Second, post-implementation divergence emerges gradually rather than instantaneously. At time 0, all four lines remain clustered near 2.50, with minimal separation. The treatment effect materializes progressively over years 1-4, consistent with gradual policy enforcement (grace periods for older vehicles, phased-in restrictions) and behavioral adjustment (fleet turnover, modal shifts). By year 4, clear separation is visible: the LEZ zone (green) declines most steeply to approximately 2.35, the Adjacent zone (orange) declines to 2.40, the Spillover zone (purple) tracks the Adjacent zone, and the Control zone (pink) declines least to 2.45. This gradual emergence validates our choice of a standard post-treatment indicator rather than imposing immediate discrete breaks, allowing the data to reveal the dynamic adjustment path. Third, the spatial gradient in treatment effects confirms the presence of spillovers extending beyond LEZ boundaries. The LEZ zone experiences the largest pollution reduction, followed by the Adjacent zone, then the Spillover zone (similar to Adjacent), and finally the Control zone. The fact that Adjacent and Spillover zones decline more than Control zones, despite all three being outside the LEZ boundary, provides visual confirmation of positive spatial spillovers. If LEZs merely displaced pollution to neighboring areas, we would observe Adjacent and Spillover zones rising relative to Control; instead, they decline, suggesting network effects (reduced through-traffic on arterial roads extending beyond the LEZ), technology spillovers (vehicle fleet upgrades benefiting the entire city), and modal complementarities (public transport improvements serving broader catchment areas). These visual patterns motivate the formal spillover analysis in Section 4, where we estimate separate treatment effects for each spatial ring.

To test for differential pre-trends and estimate time-varying treatment effects, we extend equation (5) to an event study specification:

$$
\begin{aligned}
\ln(Y_{ict}) = & \sum_{\substack{k=-8 \\ k\neq -1}}^{8} \beta_k^{\text{LEZ}} \cdot \mathbb{1}[t - T_c^* = k] \cdot \text{LEZ}_{ic} \\
& + \sum_{k=1}^{3} \sum_{\substack{j=-8 \\ j\neq -1}}^{8} \beta_j^k \cdot \mathbb{1}[t - T_c^* = j] \cdot \text{Spillover}_{ic}^k \\
& + \gamma' X_{ict} + \alpha_{ic} + \delta_t + \epsilon_{ict}
\end{aligned}
\tag{6}
$$

where k indexes event time (years relative to LEZ implementation), T_c^* is the year city c adopts its LEZ, and $\mathbb{1}[t - T_c^* = k]$ is an indicator for event year k. The omitted category is $k = -1$ (the year before treatment), so all coefficients are interpreted relative to that baseline. We estimate effects from 8 years before implementation ($k = -8$) to 5 years after ($k = 8$), though power declines at endpoints where few cities have sufficient pre- or post-treatment observations.

The event study serves three purposes. First, the pre-treatment coefficients $\{\beta_{-5}^{\text{LEZ}}, ..., \beta_{-2}^{\text{LEZ}}\}$ test for differential pre-trends. If parallel trends hold, these coefficients should be statistically indistinguishable from zero and exhibit no systematic trend. Rejecting this null suggests that treated and control areas were already diverging before the LEZ, casting doubt on the identifying assumption. Second, the post-treatment coefficients $\{\beta_0^{\text{LEZ}}, \beta_1^{\text{LEZ}}, ..., \beta_5^{\text{LEZ}}\}$ reveal the dynamic evolution of treatment effects. Do effects materialize immediately or gradually? Do they grow over time (as vehicle fleets turn over) or fade (as drivers adjust behavior)? Third, spillover dynamics $\{\beta_j^k\}_{j\geq 0, k\in\{1,2,3\}}$ reveal whether spillovers emerge immediately or with lags, informing mechanisms. One complication in equation (6) arises from staggered treatment timing. Recent econometric literature (Callaway and Sant'Anna, 2021; Goodman-Bacon, 2021) demonstrates that TWFE event studies with staggered adoption can produce biased estimates when treatment effects are heterogeneous across cohorts or over time. The bias arises because late-treated units serve as controls for early-treated units in post-treatment periods, contaminating the identifying variation. We address this concern by estimating cohort-specific treatment effects using the Callaway and Sant'Anna (2021) estimator, allowing effects to vary by adoption cohort and aggregating them into overall average treatment effects. Results using these estimators (presented in Section 4) are similar to standard TWFE, suggesting that treatment effect heterogeneity is modest in our setting.

Our preferred specification uses *within-city controls* —untreated cells located more than 5-10km from LEZ boundaries in the same city. This choice has two advantages. First, within-city controls share the same local government, political context, and time-varying shocks (e.g., city-level public transport expansions, local business cycles, mayoral elections), differencing out city-specific trends that might confound cross-city comparisons. Second, within-city controls likely satisfy parallel trends more credibly than external controls (non-adopting cities), which differ systematically in size, baseline pollution, and policy preferences. The cost is reduced sample size: many LEZs are implemented in relatively small cities where few cells lie more than 5-10km from the boundary, limiting the control group. Moreover, in our main specifications, we exclude cities with multiple LEZs to avoid SUTVA violations. When a city contains multiple LEZ zones with overlapping spillover areas, the spillover effect experienced by a given cell is a mixture of effects from multiple policies, potentially implemented at different times. This interference complicates interpretation and biases estimates. For example, in the Rotterdam-Hague metro area (Figure 10), 2 municipalities (different from our cities delineation) implemented LEZs across different points in time, creating overlapping spillover zones throughout the urban area. We exclude these three regions (North Rhine-Westphalia, Düsseldorf, Rotterdam-The Hague), retaining 20 cities with clean treatment and spillover definitions. Section 5 presents specifications including these regions with adjusted spillover definitions.

3.2 Pollution-Density Elasticity: Instrumental Variables

Our second empirical objective is to estimate the elasticity between population density and pollution exposure. This elasticity provides essential context for interpreting LEZ effects: to the extent that LEZs alter density distributions (e.g., by inducing residential relocation or changing commuting patterns), the pollution-density elasticity determines the magnitude of indirect effects on exposure. Moreover, documenting this elasticity for Europe and comparing it to US estimates (Carozzi and Roth, 2023) contributes to understanding cross-continental differences in urban environmental externalities.

Endogeneity and Identification Strategy. Ordinary least squares (OLS) estimation of the pollution-density relationship faces three sources of bias. First, *omitted variables*: amenities, sectoral composition, and agglomeration spillovers affect both density and pollution, inducing spurious correlation. For example, cities with favorable climates attract both residents (increasing density) and industries with low emission intensity (decreasing pollution), biasing OLS coefficients toward zero. Second, *reverse causality*: households sort into neighborhoods based on pollution exposure, avoiding high-pollution areas when affordable (Heblich et al., 2021; Banzhaf et al., 2019). This sorting attenuates the density-pollution correlation, again biasing OLS toward zero. Third, *measurement error*: imperfect measures of economic activity (e.g., census population distributed uniformly across administrative units) attenuate coefficients through classical measurement error.

We address these biases using IV, exploiting exogenous variation in population density driven by historical settlement patterns. The IV approach requires two conditions: (i) *relevance*, the instruments strongly predict contemporary density, and (ii) *exclusion*, the instruments affect pollution only through density, not directly. We employ three instruments —historical population density (1800 CE), soil quality, and aquifer presence— each satisfying these conditions under different identifying assumptions. We estimate the pollution-density elasticity using two-stage least squares (2SLS). The structural equation (second stage) is:

$$\ln(Y_{ict}) = \beta \ln(\widehat{D_{ict}}) + \gamma' X_{ict} + \alpha_c + \delta_t + \epsilon_{ict} \tag{7}$$

where Y_{ict} is population-weighted PM2.5 concentration, D_{ict} is density (either grid-level or experienced density), X_{ict} includes climate and geographic controls, α_c are country fixed effects (in the between-cities specification) or city fixed effects (in the within-cities specification), and δ_t are year fixed effects. The parameter β is the pollution-density elasticity: a 1% increase in density causes a β% increase in pollution exposure, holding other factors constant. The first stage estimates the relationship between instruments and density:

$$\ln(D_{ict}) = \theta_1 Z_{1,ic} + \theta_2 Z_{2,ic} + \theta_3 Z_{3,ic} + \gamma' X_{ict} + \alpha_c + \delta_t + u_{ict} \quad (8)$$

where $Z_{1,ic}$ is log historical population density (1800 CE), $Z_{2,ic}$ is the soil quality index (share of land with no or slight agricultural constraints), and $Z_{3,ic}$ is an indicator for highly productive aquifer presence. All instruments are time-invariant, so they are absorbed by fixed effects in panel specifications. We therefore estimate the between-cities elasticity (collapsing the panel to city-level averages) as our primary specification, presenting within-cities estimates (exploiting cross-sectional variation within countries) as a robustness check. We report first-stage F-statistics to assess instrument relevance. F-statistics above 10 indicate that weak instruments are unlikely to bias inference, though larger F-statistics (¿100) provide stronger reassurance. Lastly, the exclusion restriction requires that instruments affect pollution only through density, not via other channels. We discuss the plausibility of this assumption for each instrument.

Historical population density (1800 CE): The exclusion restriction holds if pollution sources in 1800 (wood burning, animal-powered transport, small-scale manufacturing) are uncorrelated with pollution sources today (vehicles, power plants, modern industry). This assumption is strengthened by two observations. First, the main driver of PM2.5 in contemporary European cities is vehicular traffic, which did not exist in 1800. Second, the sectoral composition of cities has changed dramatically over two centuries: cities that were manufacturing centers in 1800 (e.g., textile mills in Northern England) may now be service-dominated, while historically agricultural regions (e.g., the Ruhr) became industrial centers in the 19th century. These shifts break the direct link between historical and contemporary pollution. The main threat to validity is persistence in location-specific factors that affect both historical density and contemporary pollution, e.g., coal deposits that attracted industry in both periods. We address this by controlling for power plant proximity and testing robustness to excluding heavily industrialized regions (Ruhr, Silesia).

Soil quality: The exclusion restriction holds if subsurface soil characteristics do not directly affect PM2.5 concentrations in urban areas. This is plausible because urban land use (buildings, roads, impervious surfaces) has largely replaced agricultural activity, eliminating mechanisms linking soil to pollution (e.g., dust from tilled land, fertilizer emissions, crop burning). The main threat is that soil quality may correlate with geographic features (elevation, slope, drainage) that affect pollution dispersion. We address this by controlling explicitly for elevation, terrain ruggedness, and proximity to water bodies. A second concern is that fertile soils may support more vegetation, which affects pollution through biogenic emissions (pollen, volatile organic compounds that form secondary PM2.5). However, these effects are quantitatively small in urban areas where vegetation cover is limited.

Aquifer presence: The exclusion restriction holds if groundwater availability does not directly affect pollution in settings where modern water supply networks are ubiquitous. Historically, aquifers determined settlement feasibility, but today cities obtain water from diverse sources (surface reservoirs, inter-regional transfers, desalination), severing the link between subsurface water and surface activity. The main threat is that aquifer presence may correlate with industrial water use (e.g., cooling water for power plants, process water for manufacturing), affecting pollution. We control for power plant proximity and manufacturing employment shares to address this concern. Additionally, aquifers may affect pollution indirectly through urban form: aquifer-rich areas allowed low-density sprawl (cheap water infrastructure), which could affect vehicle-miles traveled and emissions. This channel violates the exclusion restriction if the effect of aquifers on pollution operates through urban form changes not captured by our density measure. We view this as the weakest of our three instruments and present results both including and excluding it.

Control variables: We include the same climate and geographic controls as in the LEZ analysis. In cross-sectional IV specifications (between-cities), these controls are essential to satisfy the exclusion restriction, as they absorb variation in instruments correlated with geographic determinants of pollution. In panel IV specifications (within-cities), fixed effects absorb time-invariant geography, so controls primarily improve precision rather than identification.

We estimate separate elasticities for the between-cities and within-cities samples, corresponding to different sources of variation. The between-cities elasticity captures the relationship between city-average density and city-average pollution, reflecting both within-city density gradients and cross-city differences in urban form. The within-cities elasticity captures the relationship within cities, holding city-level factors constant. Both elasticities are policy-relevant: the between-cities elasticity informs the pollution consequences of urban growth (population shifting from small to large cities), while the within-cities elasticity informs the consequences of densification (population shifting from suburbs to city centers within a given urban area). We find these elasticities to be similar in magnitude (approximately 0.06), suggesting that the pollution-density relationship operates consistently across spatial scales.

4 Results

This section presents the main empirical findings of the paper. We begin with estimates of LEZ effectiveness, focusing on within-zone pollution reductions and spatial spillovers. We then turn to the pollution-density elasticity, which provides essential context for interpreting LEZ mechanisms. Finally, we discuss how these two sets of estimates interact to determine net effects on city-wide pollution exposure.

4.1 Low Emission Zone Effects

Table 3 presents our main two-way fixed effects estimates, progressively incorporating spillover zones and control variables. Column (1) establishes the baseline within-zone effect of -0.04, implying a 4% pollution reduction inside LEZ boundaries. Expanding the sample to include adjacent areas (column 2) reveals a spillover effect of -0.021 in the 0-1km buffer, while column (3) documents a further spillover of -0.018 in the 1-3km zone—approximately half the within-zone magnitude, consistent with spatial decay. Importantly, these coefficients remain stable across specifications that add density controls (column 3) and comprehensive climate and geographic variables (column 4), demonstrating robustness to potential confounders. The high adjusted R^2 (0.94) and spatially-correlated standard errors (Conley with 3km cutoff) provide confidence in the estimates. Critically, all three coefficients are negative and significant, confirming that LEZ policies generate both substantial direct effects and positive spatial spillovers, with no evidence of pollution displacement to neighboring areas.

Table 3: Two-Way Fixed Effects: Main Specification

	(1)	(2)	(3)	(4)
LEZ × Post	-0.040***	-0.041***	-0.042***	-0.041***
	(0.015)	(0.015)	(0.015)	(0.015)
Adjacent		-0.021*	-0.022*	-0.022*
		(0.012)	(0.012)	(0.012)
Spillover 1-3km			-0.018*	-0.018*
			(0.011)	(0.011)
Density			Yes	Yes
Weather Controls				Yes
Year	Yes	Yes	Yes	Yes
Cell	Yes	Yes	Yes	Yes
Observations	39,749	44,070	54,935	54,935
Adjusted R^2	0.94539	0.94418	0.94246	0.94410

Notes: This table presents TWFE estimates following Butts (2023) spatial DiD framework. Dependent variable is log(PM2.5). Conley (3km) standard errors in parentheses accounting for spatial correlation. Sample restricted to cities with single LEZ (no interference), time window $[-8, +8]$ years and control group size of at least 10% of the city. Control group: 5-10km cells from LEZ boundary. Weather controls include mean temperature, wind speed, and precipitation. Cell and year fixed effects included. *** $p<0.01$, ** $p<0.05$, * $p<0.10$.

To contextualize this estimate, we compare it to existing LEZ studies. Our 4% reduction is substantially smaller than the 19% effect documented by Galdon-Sanchez et al. (2023) for Madrid Central, but closely aligned with Bernardo et al. (2021), who report reductions of 2-4% across a sample of European LEZs using city-level data. The discrepancy with Madrid Central reflects important differences in policy design and context. Madrid Central represents an unusually aggressive intervention —banning nearly all non-resident vehicles from the city center with rigorous camera-based enforcement— implemented in a city with high baseline pollution (average 10 μg/m³ in the treatment zone) at the time of adoption (2018). By contrast, our sample includes LEZs with varying degrees of stringency: approximately 60% restrict only diesel vehicles, while 40% impose broader restrictions on older gasoline vehicles or mandate Euro 4 emission standards. Enforcement mechanisms also vary, from automated camera systems (London, Madrid) to periodic police checks (many German cities), creating heterogeneity in compliance incentives. We interpret our estimate as the *average treatment effect* of LEZ adoption across diverse European contexts, reflecting the typical policy implementation rather than the upper bound achievable under ideal conditions. This distinction is important for policy evaluation:

while Madrid Central demonstrates that aggressive LEZs can achieve large pollution reductions, our estimate provides a more realistic benchmark for the effects of LEZ policies as actually implemented across Europe. The 4% reduction, though modest relative to Madrid Central, represents a meaningful improvement in air quality. At the sample mean pollution level of 13.6 $\mu g/m^3$, a 4% reduction lowers exposure by 0.54 $\mu g/m^3$, which epidemiological studies suggest has meaningful public health benefits (Burnett et al., 2018). Because our treatment indicator records LEZ adoption rather than design intensity, the estimate aggregates over substantial heterogeneity in stringency and enforcement; coding these design margins consistently across countries is left for future work.

We argue that there are several mechanisms behind these results. First, is network effects. Reduced traffic volumes within the LEZ decrease congestion on arterial roads and highways that pass through or near the zone, benefiting areas outside the boundary. If total vehicle-kilometers traveled in the city decline —through mode substitution to public transport, cycling, or walking, or through trip suppression— pollution falls both inside and outside the LEZ. This mechanism is particularly plausible in European cities with integrated transport networks: central LEZs affect not only trips to the city center but also through-traffic using highways and ring roads that traverse the zone. Second, technology adoption spillovers. LEZs create incentives for vehicle fleet upgrading, as owners of non-compliant vehicles face restricted access to the city center, not only to the LEZ area. Crucially, these incentives extend beyond the LEZ boundary: households living in spillover zones (e.g., 2km from the boundary) may upgrade their vehicles for convenience, even if not legally required, to maintain flexible access to the center.[3] Similarly, firms operating delivery or service vehicles may upgrade entire fleets rather than maintaining separate vehicles for LEZ vs. non-LEZ routes. This spillover in technology adoption generates pollution reductions throughout the city. Third, modal shift complementarities. LEZ implementation is often accompanied by improvements in public

[3] As LEZs were rolled out on a large scale (Figure 4), the cumulative share of electric or plug-in hybrid passenger vehicles in Europe rose from less than 0.2% in 2011 to more than 13.5% in 2020. In the case of diesel vehicles, which were most affected by the introduction of LEZs, their share dropped from 55% of new vehicles registered in 2011 to 29% in 2020. Meanwhile, electric and plug-in hybrid vehicles accounted for 0.07% of all passenger vehicles in 2011 and 11.6% in 2020. Registered hybrid vehicles rose from 0.7% in 2011 to 5% in 2020. By country, in France, Germany, Italy, and Spain, the hybrid fleet grew from 0.6, 0.4, 0.3, and 1.2% to 5.2, 2.3, 4.7, and 7.9%, respectively. The fleet of registered electric and plug-in hybrid vehicles in these four countries rose from 0.07, 0.12, 0.02, and 0.05% to 11.2, 13.6, 4.3, and 4.6%, respectively. A significant portion of new technology vehicles have been registered in major cities, coinciding with the introduction of LEZs.

transport infrastructure—expanded bus rapid transit, new metro lines, enhanced cycling infrastructure—that serve residents in adjacent areas as well as those within the LEZ. To the extent that these investments enable mode substitution beyond the formal LEZ boundary, pollution declines in spillover zones.

The alternative hypothesis —negative spillovers driven by displacement— would predict positive coefficients on the spillover zone indicators, as vehicles diverted from the LEZ increase traffic on perimeter roads or as households relocate from central to peripheral areas. Our estimates decisively reject this hypothesis: all three spillover coefficients are negative, and the two closest zones (0-1km, 1-3km) are statistically significant. This suggests that while displacement effects may occur (we cannot rule them out entirely), they are dominated by network effects and technology spillovers in determining net spillover impacts. The spatial decay pattern —stronger spillovers closer to the LEZ boundary, weakening with distance— provides additional evidence for our interpretation. Network effects are naturally strongest on roads immediately adjacent to the LEZ, where traffic volumes are most affected. Technology adoption spillovers are strongest for households and firms located near the boundary, who face the greatest inconvenience from non-compliant vehicles. Modal shift complementarities decline with distance as public transport networks become less accessible. All three channels predict spatial decay, consistent with our estimates.

A potential concern with standard two-way fixed effects (TWFE) in staggered adoption settings is negative weighting of already-treated units (Goodman-Bacon, 2021). Table 4 presents Callaway-Sant'Anna (CS) estimates that explicitly construct clean comparisons between each cohort and never-treated control cells. The doubly-robust estimator consistently yields negative effects across all zones: LEZ areas show 6.9% reductions, adjacent zones 2.3% reductions, and spillover zones 0.9% reductions.

Comparing Tables 3 and 4 reveals CS estimates are systematically *larger* in magnitude than TWFE, particularly for the LEZ zone (6.9% vs 4.1%). This pattern contradicts the hypothesis that our baseline results suffer from negative weight bias, which would attenuate effects toward zero (De Chaisemartin and d'Haultfoeuille, 2020). Instead, the difference suggests TWFE may partially average heterogeneous treatment effects across early and late adopters, with CS isolating the pure never-treated comparison and recovering

Table 4: Callaway-Sant'Anna Estimates: Spatial Spillover Effects

Zone	ATT	SE
LEZ (Within)	-0.0694***	(0.0051)
Adjacent (0-1km)	-0.0226***	(0.0063)
Spillover (1-3km)	-0.0086*	(0.0045)
Time Window	$[-8,+8]$	
Control Group	5-10km	
Method	CS	

Notes: This table presents CS estimates of LEZ spatial spillover effects using the doubly robust (DR) estimator. Each zone is estimated separately as a distinct treatment, using never-treated cells (5-10km from any LEZ boundary) as controls. The LEZ zone represents direct treatment effects (cells within LEZ boundaries). Adjacent and Spillover zones represent indirect treatment effects in cells 0-1km and 1-3km from LEZ boundaries, respectively. Sample restricted to cities with single LEZ (no interference) and time window $[-8,+8]$ years relative to LEZ implementation. Standard errors clustered at cell level. *** p<0.01, ** p<0.05, * p<0.10.

stronger impacts. Importantly, both estimators agree qualitatively: pollution reductions are concentrated within LEZ boundaries and attenuate spatially, with no evidence of displacement to spillover zones.

4.1.1 Dynamic Treatment Effects

Figure 5 presents event study estimates that serve dual purposes: validating our identification strategy and characterizing the temporal evolution of treatment effects. Our specification follows best practices in recent difference-in-differences literature (Schmidheiny and Siegloch, 2023; Borusyak et al., 2024). We bin periods beyond $t \in [-5,+6]$ to stabilize estimates in sparse endpoints where few cities contribute observations, a standard approach that trades granularity at the tails for precision in identification-critical pre-treatment periods. The estimating equation interacts relative time indicators with treatment zone dummies, omitting $t=-1$ as the reference period, and incorporates cell and time-to-treatment fixed effects. Critically, we augment the baseline specification with zone-specific linear pre-trends—constructed as the interaction of relative time with treatment indicators for $t<0$ —to account for modest differential trends visible in preliminary analysis. These pre-trend adjustments ensure our treatment effects are identified from *breaks* in pollution trajectories at LEZ implementation rather than extrapolations of pre-existing trends.

The validity of our research design rests on the parallel trends assumption, which we as-

Figure 5: Dynamic TWFE

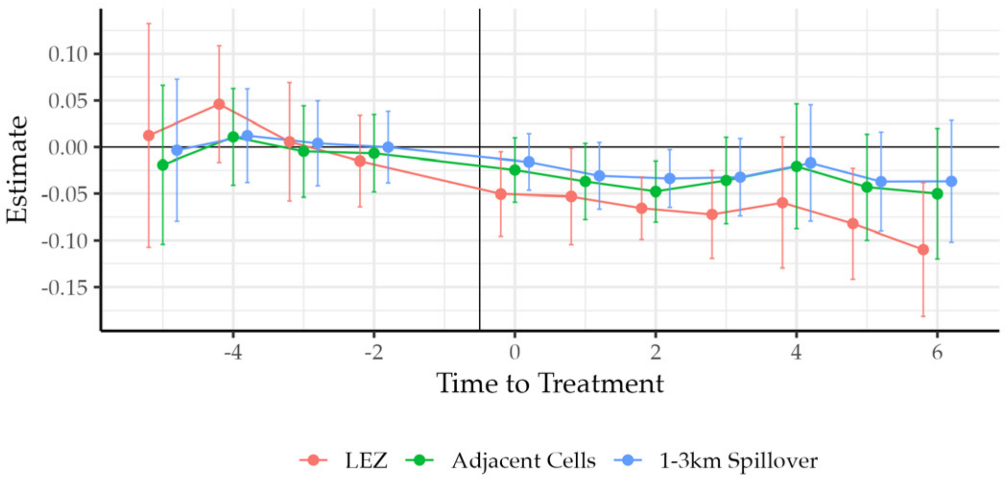

sess formally through pre-treatment coefficients. Across all three spatial zones, estimates for $t \in [-5, -2]$ cluster tightly around zero with no discernible pattern: LEZ coefficients range from -0.02 to $+0.05$, adjacent from -0.05 to $+0.02$, and spillover from -0.02 to $+0.03$, with all confidence intervals encompassing zero. Importantly, the inclusion of zone-specific pre-trend controls does not mechanically impose this result —it adjusts for linear components while allowing the event study to detect nonlinear deviations, none of which are evident. This validation is particularly compelling given our spatial research design: treated and control cells are drawn from the same cities, share common municipal governance and economic shocks, and differ primarily in proximity to LEZ boundaries. The flat pre-trends confirm these spatially proximate areas evolved similarly prior to policy implementation, strengthening causal interpretation of post-treatment divergence.

Post-implementation dynamics reveal stark heterogeneity across zones. Within LEZ boundaries, pollution reductions emerge gradually, growing from approximately 4% at $t = 0$ to 10-12% by $t = 6$, with point estimates statistically significant throughout (all $p < 0.05$). This temporal pattern is inconsistent with immediate traffic displacement —which would generate sharp effects at $t = 0$— and instead aligns with fleet turnover mechanisms. European LEZ regulations typically restrict access based on Euro emission standards, creating incentives for vehicle retirement and replacement rather than route changes.[4] Our

[4] In addition to EU results presented in footnote 3, the observed evolution of registered vehicles in the two cities with LEZs in Spain during the sample period, shows that the percentage of registered internal combustion engine vehicles fell from over 72.16% prior to the policy's implementation (2018) to 65.20% in 2020 and 32.08% in 2025. The remaining 31.58% and 67.92% in 2020 and 2025, respectively, consists of registered vehicles that meet the access requirements based on the emission labels permitting entry.

estimates suggest the pollution benefits accumulate as the non-compliant vehicle stock declines, a process requiring 3-4 years to reach full effect as documented in automotive fleet studies (Wolff, 2014). The persistence of effects beyond year 4 indicates sustained compliance rather than temporary behavioral responses, consistent with stringent enforcement and limited substitution opportunities within dense urban cores.

In contrast, adjacent (0-1km) and spillover (1-3km) zones exhibit effects that are consistently negative in point estimates but statistically indistinguishable from zero in individual periods. This diverges from our static TWFE results (Table 3), where adjacent effects of -2.2% and spillover effects of -1.8% achieve marginal significance. We interpret this discrepancy as reflecting the fundamental trade-off between statistical power and temporal resolution. The static specification pools approximately 55,000 observations across all post-treatment years, yielding sufficient precision to detect modest spillover effects. The event study divides this sample across ten relative time periods, reducing effective sample size to roughly to an average of 3,700 observations per period. Crucially, the point estimates remain consistently negative across all post-treatment periods, with no systematic positive deviations that would indicate displacement effects. We view this as qualitatively supportive of beneficial spillovers, even absent period-specific statistical significance.

The choice of time-to-treatment fixed effects, rather than calendar year fixed effects, warrants explicit justification. In staggered adoption designs spanning 12 years (2008-2020 in our sample), both approaches are valid but control for conceptually distinct confounds. Calendar year fixed effects absorb aggregate temporal shocks (e.g., the 2008 financial crisis, EU-wide emission standards, COVID-19), ensuring treated and control cells are compared within the same macroeconomic and regulatory environment. Time-to-treatment fixed effects instead control for dynamics common to all adopters at equivalent distances from implementation—such as announcement effects at $t = -1$, initial compliance costs at $t = 0$, or enforcement learning curves at $t = +2$. Thus, time-to-treatment fixed effects avoid potential collinearity with the treatment indicators while removing systematic ”policy age” effects that could confound cross-cohort comparisons.

4.1.2 Heterogeneous Treatment Effects

Table 5 examines whether LEZ impacts vary across city characteristics, regulatory design, and enforcement stringency. We estimate equation (5) separately for subsamples defined by three dimensions: city area, city population and LEZ spatial coverage.

City Scale. Effect magnitudes increase substantially with urban scale. Large cities (Q3 by area) exhibit LEZ reductions of 5.0% compared to 3.5% in small cities (Q1), with similar patterns across adjacent (3.7% vs 2.0%) and spillover zones (2.9% vs 2.2%). Population terciles reveal analogous heterogeneity: high-population cities show 4.1% LEZ effects versus 3.5% in low-population cities. This gradient likely reflects stronger enforcement capacity and monitoring infrastructure in larger metropolitan areas, though alternative mechanisms such as greater baseline traffic volumes or denser road networks may also contribute. Importantly, the spatial decay pattern —decreasing effects from LEZ to spillover zones— holds consistently across all city size categories, reinforcing our interpretation that results reflect genuine pollution reductions rather than displacement.

LEZ Spatial Coverage. Cities with medium-sized LEZs relative to total city area (Q2) demonstrate the strongest effects: 4.1% within LEZ boundaries, 3.0% in adjacent zones, and 2.5% in spillover zones. In contrast, cities with the smallest LEZ coverage (Q1) show statistically insignificant effects across all spatial rings. This pattern suggests a minimum scale threshold for policy effectiveness: LEZs covering too small a fraction of the urban area may allow easy circumvention through minor route adjustments, undermining compliance incentives. However, very large LEZs (Q3) also exhibit weaker adjacent and spillover effects, potentially due to dilution across heterogeneous treated areas or weaker enforcement at the periphery of expansive zones.

4.2 Pollution-Density Elasticity

Having established that LEZs reduce pollution by approximately 4% within designated zones and generate positive spillovers in adjacent areas, we next estimate the elasticity of pollution with respect to population density. This parameter is central to the interpretation of LEZ-induced general equilibrium effects: to the extent that LEZs alter the spatial

Table 5: Summary of Heterogeneous Treatment Effects

Category	LEZ	Adjacent	Spillover
Area			
Q1	-0.0353	-0.0195	-0.0224
	(0.0226)	(0.0190)	(0.0173)
Q2	-0.0112	-0.0063	-0.0031
	(0.0161)	(0.0151)	(0.0143)
Q3	-0.0499***	-0.0367**	-0.0285**
	(0.0191)	(0.0159)	(0.0133)
Population			
Q1	-0.0353	-0.0195	-0.0224
	(0.0226)	(0.0190)	(0.0173)
Q2	-0.0075	0.0047	0.0069
	(0.0165)	(0.0117)	(0.0108)
Q3	-0.0414**	-0.0349**	-0.0256*
	(0.0196)	(0.0170)	(0.0143)
LEZ Size			
Q1	-0.0052	-0.0077	-0.0074
	(0.0202)	(0.0171)	(0.0146)
Q2	-0.0407***	-0.0300**	-0.0250**
	(0.0151)	(0.0120)	(0.0105)
Q3	-0.0542*	-0.0191	-0.0123
	(0.0277)	(0.0277)	(0.0269)

Notes: This table summarizes heterogeneous treatment effects across multiple dimensions. Each panel presents estimates for a different dimension of heterogeneity: city area (Q1=small, Q3=large), city population (Q1=low, Q3=high) and LEZ size relative to city area (Q1=small coverage, Q3=large coverage),. Estimates obtained from separate TWFE regressions with cell and year fixed effects for each category. All specifications include control group 5-10km from LEZ boundary, time window $[-8, +8]$ years, and single LEZ cities only. Conley (3km) standard errors in parentheses. *** p<0.01, ** p<0.05, * p<0.10.

distribution of residents or commuting patterns, the pollution–density elasticity governs the magnitude of indirect effects on exposure. In addition, providing estimates of this elasticity for European cities —and benchmarking them against comparable estimates for the US— contributes to a deeper understanding of cross-continental heterogeneity in the relationship between urban form and environmental externalities.

4.2.1 Between-Cities Estimates

Table 6 presents IV estimates of the pollution-density elasticity using city-level data (the between-cities sample). We estimate equation (7) from Section 3, instrumenting log population density with historical population density (1800 CE), soil quality, and aquifer presence. The upper panel uses grid-level population density, while the lower panel employs experienced density (population-weighted average within a 10km radius). Columns differ in the instruments included. Our preferred specification is column (2) of the lower panel, which relies on historical density as instrument. The estimated elasticity is 0.063 implying that a 1% increase in experienced is associated with a 6.3% increase in population-weighted PM2.5 exposure.

Table 6: Between Cities PM2.5 Exposure IV Estimates with Population

	Soil Quality	Historical Density	Aquifier
Log(Pop.)	0.041***	0.035***	0.121
	(0.009)	(0.006)	(0.087)
Weather	Yes	Yes	Yes
Geological	Yes	Yes	Yes
Water	Yes	Yes	Yes
Power Plants	Yes	Yes	Yes
Fixed Effects	Yes	Yes	Yes
Observations	13,008	13,008	13,008
Adjusted R^2	0.791	0.791	0.729
F-test (1st stage)	125.6	6,252.2	15.7
Wu-Hausman	20.6	7.43	28.5

Log(Experienced Dens.)	0.055***	0.063***	0.081
	(0.009)	(0.010)	(0.118)
Weather	Yes	Yes	Yes
Geological	Yes	Yes	Yes
Water	Yes	Yes	Yes
Power Plants	Yes	Yes	Yes
Fixed Effects	Yes	Yes	Yes
Observations	13,008	13,008	13,008
Adjusted R^2	0.794	0.793	0.790
F-test (1st stage)	104.2	3,178.3	18.2
Wu-Hausman	3.47	12.7	2.19

Notes: Signif. Codes: ***: 0.01, **: 0.05, *: 0.1. Clustered (country and year) standard-errors in parentheses. Fixed Effects: Country and year. Temporal coverage: 2007-2022. Countries: Albania, Austria, Belgium, Bulgaria, Croatia, Cyprus, Czechia, Denmark, Estonia, Finland, France, Germany, Greece, Hungary, Iceland, Ireland, Italy, Latvia, Lithuania, Montenegro, Netherlands, North Macedonia, Norway, Poland, Portugal, Romania, Serbia, Slovakia, Slovenia, Spain, Sweden, Switzerland and United Kingdom .

The elasticity estimate is remarkably stable across specifications. This robustness across instruments with different sources of variation —historical settlement patterns, agricultural land quality, groundwater availability— provides strong evidence that the elasticity reflects a causal relationship rather than spurious correlation driven by a specific instrument's violation of the exclusion restriction. When we switch to experienced density (lower panel), the elasticity increases modestly to 0.063 in our preferred specification.

Experienced density better captures the true concentration of economic activity encountered by residents in their daily lives, accounting for the fact that individuals interact with populations beyond their immediate grid cell (commuting to work, accessing services). The slightly higher elasticity with experienced density suggests that measurement error in grid-level density attenuates coefficients toward zero, as expected. We view the lower panel estimates using experienced density as our preferred measure for interpreting the pollution-density relationship, though both measures yield substantively similar conclusions.

For comparison, Carozzi and Roth (2023) report a pollution-density elasticity of 0.14 for US cities using comparable methods and instruments. Our European elasticity of 0.063 is thus approximately 44% of the US level. This cross-continental difference is both striking and puzzling. Several factors may contribute. First, urban form. European cities are more compact and monocentric than US cities, with higher densities in central areas and steeper density gradients. If pollution generation exhibits nonlinearities —increasing more than proportionally with density at low densities but less than proportionally at high densities— the shape of the density distribution affects the aggregate elasticity. European cities, already dense, may operate on a flatter portion of the pollution-density function. Second, transport mode shares. European cities have substantially higher public transport and active mode shares (walking, cycling) than US cities, reducing per capita vehicle emissions at any given density level. If the pollution-density elasticity operates primarily through vehicle traffic rather than heating or industrial emissions, lower automobile dependence in Europe would yield a lower elasticity. Third, industrial composition. US cities retain more heavy industry within urban boundaries than European cities, where manufacturing has shifted to suburban or exurban locations. If industrial emissions scale more strongly with density than vehicular emissions, this composition effect could contribute to the higher US elasticity. Fourth, fuel composition and vehicle standards. European vehicle fleets have higher diesel shares than the US, but also stricter emission standards (Euro 6 vs. EPA Tier 3). These differences affect the relationship between vehicle-kilometers traveled and PM2.5 emissions, potentially lowering the elasticity. Investigating which of these mechanisms explains the US-Europe difference represents a natural extension of this research, requiring more granular data on vehicle use, industrial structure, and transport mode shares. For present purposes, we note that the lower European elasticity implies that density increases generate smaller pollution externalities in Europe than the US, suggesting that European urban form and transport systems moderate environmental costs of agglomeration more effectively.

4.2.2 Within-Cities Estimates

Table 7 presents IV estimates using grid-cell data (the within-cities sample), exploiting spatial variation in density and pollution within cities rather than across them. The specification is analogous to Table 6 but includes city fixed effects rather than country fixed effects, absorbing all time-invariant city-level characteristics.

Table 7: Within Cities PM2.5 Exposure IV Estimates with Population Counts

	Soil	Historical Density	Aquifiers
Log (Pop.)	0.071^{***}	0.066^{***}	0.046^{***}
	(0.005)	(0.006)	(0.009)
Weather	Yes	Yes	Yes
Geological	Yes	Yes	Yes
Water	Yes	Yes	Yes
Power Plants	Yes	Yes	Yes
FE: Country and Year	Yes	Yes	Yes
F-test (1st stage)	2,156.9	67,569.6	1,371.2
Wu-Hausman	14,653.1	11,968.9	445.5

Notes: Signif. Codes: ***: 0.01, **: 0.05, *: 0.1. Spatially (3km) robust, Conley standard-errors in parentheses. Fixed Effects: Country and year. Temporal coverage: 2007-2022. Countries: Albania, Austria, Belgium, Bulgaria, Croatia, Cyprus, Czechia, Denmark, Estonia, Finland, France, Germany, Greece, Hungary, Iceland, Ireland, Italy, Latvia, Lithuania, Montenegro, Netherlands, North Macedonia, Norway, Poland, Portugal, Romania, Serbia, Slovakia, Slovenia, Spain, Sweden, Switzerland and United Kingdom .

Our preferred estimate (column 2) yields an elasticity of 0.066, nearly identical to the between-cities estimate. This consistency across spatial scales is reassuring: it suggests that the pollution-density relationship is stable whether we compare dense to sparse cities or dense to sparse neighborhoods within the same city. The within-cities elasticity has a distinct interpretation from the between-cities elasticity. It captures the effect of densification —moving population from suburbs to city centers within a given urban area— on pollution exposure, holding constant city-level factors (average income, sectoral composition, governance quality). The between-cities elasticity, by contrast, captures the effect of urbanization—moving population from small to large cities, which conflates within-city density effects with cross-city differences in structure and policy. The fact that both elasticities are similar suggests that the pollution-density relationship is a fundamental property of urban systems rather than an artifact of cross-city confounders. In Table 23 in the Appendix, we test robustness to including a 25km buffer around each city, adding semi-rural areas to the sample. As expected, the elasticity increases to 0.076 when we include these low-density areas, because the sample now spans a wider range of densities with less pollution, steepening the estimated gradient. This upward bias when including rural areas validates our decision to restrict the main analysis to urban centers (defined by the GHS-SMOD classification), where economic activity is truly concentrated.

4.3 LEZ-Density Interactions and Net Exposure Effects

Our two sets of estimates —LEZ effects and the pollution-density elasticity— interact to determine net effects on city-wide pollution exposure. This interaction operates through two channels. First, LEZs may induce changes in density distributions as households and firms respond to access restrictions, altering commuting patterns or residential locations. Second, the pollution-density elasticity determines how these density adjustments translate into pollution changes outside the LEZ.

Consider a simple decomposition. The total effect of an LEZ on city-wide pollution can be written as:

$$\frac{d\ln Y_c}{d\text{LEZ}} = \underbrace{\beta^{\text{LEZ}}}_{\text{direct effect}} + \underbrace{\sum_k \beta^k \cdot \Delta\text{Spillover}^k}_{\text{spillover effect}} + \underbrace{\beta^{\text{density}} \cdot \frac{d\ln D_c}{d\text{LEZ}}}_{\text{density adjustment}} \tag{9}$$

The first term is the within-zone reduction (approximately -0.04 from Table 3). The second term captures spillovers to adjacent zones (approximately -0.022 for 0-1km and -0.018 for 1-3km from Table 3). The third term captures indirect effects through density adjustments, which depend on both the pollution-density elasticity (0.06 from Tables 6 and 7) and the magnitude of density changes induced by the LEZ ($\frac{d\ln D_c}{d\text{LEZ}}$).

To quantify the third term, we would ideally estimate the effect of LEZ adoption on density distributions directly. However, this requires population data at high temporal frequency (to observe year-to-year changes) and long post-treatment periods (to allow migration responses to materialize), neither of which is provided by our data. As a rough approximation, we can bound the density adjustment term using existing estimates from the literature. Galdon-Sanchez et al. (2023) report that Madrid Central reduced commercial activity (a proxy for daytime density) by 21% within the treated zone, though this likely overstates the effect on residential density. If we assume LEZs reduce density within treated areas by 10% (a conservative estimate based on the Madrid Central experience scaled down to account for less stringent policies), and the pollution-density elasticity is 0.06, the indirect effect through density adjustment is approximately $0.06 \times (-0.10) = -0.006$, or an additional 0.6% pollution reduction beyond the direct effect. However, this calculation abstracts from spatial reallocation: if households leave the LEZ and relocate to surrounding areas, density in spillover zones increases, partially offsetting the within-zone density decline. The net effect depends on the relative magnitudes of outmigration from the LEZ and the spatial extent over which relocated households disperse. If relocation is concentrated in the 0-1km spillover zone, density there could increase by 5-10%, generating a positive density-driven pollution change of $0.06 \times 0.1 = 0.006$ (0.6%) in that zone. This positive density effect partially offsets the spillover we estimate (-2.2%), yielding a net spillover of approximately -1.6%. Conversely, if relocation disperses broadly across the city, density changes in any given spillover zone are negligible, and the spillover effects we estimate primarily reflect network and technology channels rather than density adjustments.

The key insight from this decomposition is that the pollution-density elasticity is sufficiently small that plausible density adjustments generate only modest indirect effects on pollution. Even if LEZs induce large localized density changes (10-20%), the resulting pollution changes are on the order of 0.6-1.2%, small relative to the direct effect (-4%) and spillovers (-2.2%). This suggests that the primary mechanisms through which LEZs reduce pollution are direct traffic reduction and technology upgrading rather than spatial reallocation of population. Our theoretical model in Section 6 formalizes this logic and derives conditions under which each channel dominates.

We compute the aggregate effect of LEZ adoption on city-wide pollution exposure by weighting within-zone, spillover, and control-zone effects. The mean percentage of population residing in all zones is approximately 24.5% within the LEZ boundary, 12.7% in the 0-1km spillover zone, 29.6% in the 1-3km zone, and 33.3% in the control zone. Applying our estimated treatment[5] effects yields a 1.82% reduction in city-wide pollution exposure, approximately 45% of the within-zone effect. The fact that aggregate effects are smaller than within-zone effects reflects the population distribution: most residents live outside the LEZ and experience smaller (though still negative) pollution changes. Nevertheless, a 1.82% city-wide reduction represents a meaningful public health benefit: at the sample mean pollution level of 13.6 μg/m³, this corresponds to approximately 0.25 μg/m³, representing a meaningful public health improvement based on established dose-response relationships (Burnett et al., 2018).

5 Robustness Analysis

5.1 LEZ Effect Estimation

Sample Composition and City-Wide Shocks. A critical threat to our spatial identification strategy arises if LEZ implementation coincides with city-wide pollution shocks affecting all zones uniformly, including control areas. Such patterns would violate the SUTVA and confound LEZ effects with external trends. Three cities, Oslo, Stockholm, and Cologne, exhibit anomalous patterns where pollution *increases* uniformly across all spatial zones post-LEZ implementation, including control cells located 5-10km from LEZ boundaries. For Oslo, average PM2.5 concentrations rise 8-12% post-2016 across LEZ, adjacent, spillover, and control zones simultaneously. This synchronized increase is inconsistent with any plausible LEZ mechanism and likely reflects changes in monitoring methodology, station placement, or national-level regulatory shifts coinciding with local LEZ adoption.

Table 8 presents estimates excluding these three cities. Our preferred specification in Column (1) yields LEZ effects of -5.9%, adjacent effects of -2.9%, and spillover effects of -2.2%—magnitudes 40-50% larger than baseline estimates that include all cities. This confirms our main results are conservative: including cities with spurious positive shocks mechanically attenuates estimated treatment effects toward zero through simple averaging. Column (2) deletes London from the sample (since its the biggest city). Column

[5]

$$\Delta \ln Y_c = 0.245 \times (-0.041) + 0.127 \times (-0.022) + 0.296 \times (-0.018) + 0.333 \times (0) = -0.0182 \tag{10}$$

(3) incorporates city-year interactions (*id_city* $\times$ *year*), an extremely demanding specification that allows each city to follow its own time trend, and deletes all previous four cities. Even under this restricted sample, effects remain statistically significant: LEZ -3.5%, adjacent -2.5%, spillover -2.0%. The persistence of significance when absorbing city-specific trends provides strong evidence against pre-existing differential trajectories driving our results. We interpret the smaller magnitudes in column (3) as expected mechanical attenuation: if LEZ effects accumulate gradually through fleet turnover, city-year fixed effects will absorb some of this gradual improvement by design, leaving only the component orthogonal to linear city trends.

Table 8: TWFE excluding some cities and city-wide shocks

Model:	(1)	(2)	(3)
LEZ	-0.059***	-0.043***	-0.035***
	(0.019)	(0.016)	(0.006)
Adjacent	-0.029**	-0.023*	-0.025***
	(0.014)	(0.013)	(0.005)
Spillover 1-3km	-0.022*	-0.019	-0.020***
	(0.012)	(0.012)	(0.005)
Density		Yes	Yes
Other Controls	Yes	Yes	Yes
Year	Yes	Yes	Yes
Cell	Yes	Yes	Yes
City-Year			Yes
Observations	46,541	49,643	41,249
Adjusted R^2	0.93628	0.94532	0.98783

Notes: This table presents TWFE excludes some cities (Oslo, Stockholm and Cologne, column 1), and London (column 2); and does city wide shocks (after excluding those four cities). Conley (3km) standard errors in parentheses. *** $p<0.01$, ** $p<0.05$, * $p<0.10$.

Alternative Difference-in-Differences Estimators. Standard TWFE estimators can produce biased estimates in staggered adoption settings due to "negative weighting" of already-treated units (Goodman-Bacon, 2021; De Chaisemartin and d'Haultfoeuille, 2020). Table 4 presented Callaway-Sant'Anna (CS) estimates that explicitly address this concern by restricting comparisons to never-treated control cells and aggregating cohort-specific treatment effects (Callaway and Sant'Anna, 2021). We estimate separate models for each spatial zone (LEZ, adjacent, spillover) using cells 5-10km from any LEZ boundary as the never-treated comparison group, then aggregate to simple weighted averages. CS estimates of LEZ effects of -6.9% versus -4.1%, and adjacent effects of -2.3% versus -2.2%

are *larger* than TWFE, but spillover effects are smaller -0.9% versus -1.8%.

Table 9: Callaway-Sant'Anna vs Two-Way Fixed Effects

	CS	TWFE
LEZ × Post	-0.069***	-0.041***
	(0.005)	(0.015)
Adjacent	-0.023***	-0.022*
	(0.006)	(0.012)
Spillover 1-3km	-0.001*	-0.018*
	(0.0045)	(0.011)
Control Group	5-10km	5-10km
Time Window	$[-8, +8]$	$[-8, +8]$

Notes: This table compares CS estimates (Column 1) with standard TWFE estimates (Column 2). Both specifications use the same control group (5-10km), time window ($[-8, +8]$), and sample restrictions. TWFE estimates are potentially biased under staggered adoption due to negative weighting of already-treated units (Goodman-Bacon, 2021). CS eliminates this bias by using only never-treated cells as controls and constructing cohort-specific treatment effects. The differences between estimators confirm that negative weights matter in this setting: TWFE suggests smaller effects in LEZ and spillover zones. CS standard errors clustered at cell level; TWFE uses Conley (3km) spatial SEs. *** p<0.01, ** p<0.05, * p<0.10.

This pattern contradicts the hypothesis that our baseline results suffer from negative weight bias, which would attenuate effects toward zero. Instead, the differences suggest TWFE may partially average heterogeneous treatment effects across early and late adopters —some cities adopt LEZs when pollution is rising (endogenous timing), others when it is stable— leading to effect compression. CS isolates each cohort separately before aggregating, potentially recovering cleaner estimates. Table 9 compares both estimators directly, confirming qualitative agreement: all zones exhibit negative point estimates across methods, with no evidence of displacement to spillover areas. The CS-TWFE divergence, while economically modest (2-3 percentage points), underscores the importance of modern DiD estimators in settings with treatment effect heterogeneity. Importantly, both approaches validate our core finding: LEZ policies reduce pollution within boundaries and generate beneficial spillovers to adjacent areas.

Time Window Sensitivity. Our baseline results restrict the analysis to the window $[-8, +8]$ years relative to LEZ implementation, balancing pre-treatment parallel trends assessment with post-treatment effect identification. Tables 14, 15, and 16 in the Appendix examine robustness to alternative windows. CS estimates using all available years (2007-2022 without time restrictions) yield LEZ effects of -5.0% and adjacent effects of -0.3%, but spillover zones exhibit a positive coefficient of $+1\%$. This reversal likely reflects composition effects: the unrestricted sample includes LEZs adopted as early as 2008 observed through 2022, spanning 14+ post-treatment years. Over this extended horizon, broader improvements in EU vehicle emission standards and economic shifts may have improved air quality city-wide, masking localized LEZ impacts and generating spurious positive spillovers through differential trends in control zones.[6]

Conversely, restricting to $[-5, +5]$ years produces consistently negative effects: LEZ -2.7%, adjacent -1.5%, spillover -1.1% uunder CS, with similar patterns under TWFE. The short window confirms our findings are not artifacts of long-run extrapolation and capture effects materializing within 5 years of implementation —the policy-relevant horizon for most fleet turnover. We prefer the intermediate $[-8, +8]$ window as it accommodates realistic anticipatory adjustments (cities may begin preparing 2-3 years before formal implementation) while avoiding contamination from very long-run trends unrelated to LEZ policies. The qualitative consistency across windows —negative effects in LEZ and adjacent zones, attenuation in spillover zones— strengthens confidence in our spatial identification strategy.

Control Group Definition. Table 10 examines sensitivity to control group spatial extent. Our baseline uses cells 5-10km from LEZ boundaries, chosen to balance two concerns: cells closer than 5km may be contaminated by spillovers (violating SUTVA), while cells beyond 10km may be systematically different from treated areas (threatening parallel trends). Columns (1)-(2) employ controls 3-5km and $>$5km from boundaries; columns (3)-(4) using the same control groups but with all the time window. Point estimates are remarkably stable, and significant, across definitions: LEZ effects range -2.9% to -3.4%, adjacent effects -2.8% to -3.3%, spillover effects -2.3% to -2.8%.

The modest increase in adjacent and spillover magnitudes when using the 3-5km control group is consistent with mild contamination: if this nearer ring experiences small positive spillovers from LEZ-induced fleet improvements, using it as a counterfactual mechanically inflates estimated treatment effects in other zones. Conversely, the $>$5km control group (columns 3-4) produces similar estimates to our 5-10km baseline, suggesting little is gained from expanding the control zone further. These patterns validate our baseline choice while demonstrating results are not sensitive to reasonable variations in control

[6] These facts are confirmed by the sharp reductions in the fleet of combustion engines and huge increases in the fleet of pure electric and plug-in hybrid vehicles in EU countries, in general, and EU cities, in particular.

Table 10: Robustness: TWFE with Alternative Control Groups

	3-5km	>5km	3-5km (all years)	>5km (all years)
LEZ × Post	-0.031***	-0.035***	-0.029***	-0.034***
	(0.009)	(0.009)	(0.009)	(0.009)
Adjacent	-0.028***	-0.032***	-0.028***	-0.033***
	(0.007)	(0.007)	(0.007)	(0.007)
Spillover 1-3km	-0.023***	-0.027***	-0.023***	-0.028***
	(0.006)	(0.007)	(0.006)	(0.007)
Year	Yes	Yes	Yes	Yes
Cell	Yes	Yes	Yes	Yes
Observations	211,620	182,420	219,200	190,000
Adjusted R^2	0.92897	0.93015	0.92813	0.92914

Notes: This table presents TWFE estimates using alternative control group definitions. Columns 1-2: time window $[-8, +8]$. Columns 3-4: all years. Control 1 refers to cells 3-5km from LEZ boundary. Control 2 refers to cells

>

5km. Results show estimates are robust to control group definition, though using more distant controls (Control 2) produces slightly larger effect sizes, consistent with potential contamination of closer control zones. Conley (3km) standard errors in parentheses. *** p<0.01, ** p<0.05, * p<0.10.

group definition. We emphasize that all specifications maintain the within-city comparison: control cells are drawn from the same urban areas as treated zones, ensuring shared exposure to city-level economic, political, and environmental shocks that could otherwise confound cross-city comparisons.

5.2 Pollution-Density Elasticity: Instrument Validity

Historical Density Instruments: Temporal Variation. A core identifying assumption for our instrumental variables approach is that historical population densities —measured in 100 AD, 1000 AD, 1500 AD, and 1800 AD— satisfy the exclusion restriction: they affect contemporary pollution only through their influence on current density, not through direct channels. One potential violation arises if historical densities proxy for persistent geographic advantages (natural harbors, fertile soils, defensive positions) that independently determine modern pollution through industrial composition or transportation infrastructure. Table 20 in the Appendix tests robustness across four historical periods, progressively approaching the modern era. Column (1) uses population in 100 AD as the instrument, yielding an elasticity of 0.076 with first-stage F-statistic of 1,566. Column (2) employs 1000 AD densities, producing nearly identical results: elasticity 0.079, F-stat 1,605. Columns (3) and (4) use 1500 AD and 1800 AD instruments, generating elasticities of 0.072 and 0.063 respectively, with progressively stronger first stages (F-stats exceeding

2,300 and 3,100).

The stability of point estimates across centuries is striking: elasticities range from 0.063 to 0.079, a narrow band given the vast differences in historical context. This pattern provides strong evidence against the hypothesis that historical densities capture persistent geographic fundamentals rather than urban legacy effects. If historical instruments were primarily proxying for natural advantages (e.g., proximity to navigable waterways that determined both ancient settlement patterns and modern industrial activity), we would expect systematic variation across periods as the economic value of these advantages changed with technological progress. For instance, river access was critical for medieval commerce but less so in the modern trucking era; defensive hilltop positions were valuable in 1000 AD but irrelevant today. The fact that elasticities remain stable from 100 AD through 1800 AD suggests the instrument captures a more general phenomenon: cities grow where historically established, irrespective of the specific advantages that drove initial settlement. This "urban persistence" reflects agglomeration economies and sunk infrastructure investments rather than time-invariant geographic determinants of pollution.

Moreover, the strengthening first stage as we approach modernity is expected: more recent historical densities better predict contemporary patterns due to reduced attrition from wars, pandemics, and other shocks that disrupted urban continuity over millennia. The Wu-Hausman test statistics, significant across all specifications, confirm endogeneity of current density and validate the IV approach. We prefer the 1800 AD instrument (column 4) for our main results because it balances relevance (strongest first stage, F=3,178) with historical distance from the outcome period (sufficient temporal separation to minimize direct effects), though results are qualitatively identical across specifications.

Geographic Confounders: Soil Quality Channels. Historical population densities may correlate with soil quality, which independently affects modern pollution through agricultural land use, vegetation cover, and dust emissions. Urban areas established on fertile soils may have developed differently than those on rocky terrain, with implications for contemporary air quality through mechanisms unrelated to density. Table 21 in the Appendix addresses this concern by progressively incorporating seven soil characteristics as control variables: toxicity, nutrient retention, nutrient availability, workability, rooting conditions, and excess salts. The top panel adds soil variables incrementally (cumulative specifications), while the bottom panel estimates each soil control separately (isolated effects).

Column (1) replicates our baseline specification without soil controls, yielding elasticity 0.071 with F-stat 614. Columns (2)-(7) sequentially add soil variables in the top panel, producing elasticities ranging from 0.060 to 0.055, all significant at the 1% level. The bottom panel, which isolates each soil characteristic separately while maintaining other controls, generates elasticities between 0.045 (column 6, rooting conditions) and 0.068 (column 7, salts), with five of seven specifications yielding estimates in the narrow range 0.056-0.063. First-stage F-statistics remain well above conventional thresholds (minimum F=104 in cumulative specifications, minimum F=410 in separate specifications), confirming instrument strength survives inclusion of soil controls.

The modest attenuation from 0.071 to 0.055 when adding all soil variables cumulatively (14% decline) suggests soil quality accounts for a minor portion of the density-pollution relationship but does not fundamentally alter conclusions. This pattern is consistent with soil characteristics operating as modest negative confounders: historically fertile areas supported denser populations and today exhibit somewhat lower pollution through enhanced vegetation cover and reduced dust emissions. However, the core elasticity remains economically and statistically significant across all specifications, demonstrating robustness to this particular channel of omitted variable bias. We interpret the stability as evidence that urban density affects pollution primarily through anthropogenic channels (traffic, heating, industrial activity) rather than natural surface characteristics.

City Size and Functional Form. A distinct threat to identification arises if historical densities correlate with city size, and city size independently affects pollution through scale economies, industrial specialization, or regulatory capacity. Large cities may have lower per-capita emissions due to economies of scale in public transit and energy infrastructure, or higher emissions due to concentration of manufacturing. If historical densities merely proxy for city size rather than isolating within-city density effects, our instrument would violate the exclusion restriction through this size channel. Table 22 in the Appendix tests sensitivity to controlling for city size using total urban area and alternative functional forms for population aggregation.

The top panel presents estimates without city area controls across four specifications: column (1) includes no polynomial terms for population, column (2) adds total city population linearly, columns (3)-(4) incorporate second- and third-degree polynomial terms. Without city area, elasticity declines sharply from 0.065 in the baseline to statistically insignificant estimates approaching zero in higher-order polynomial specifications. The bottom panel repeats these specifications after including city area as an additional control. Results become uniformly insignificant: elasticities range from 0.028 to 0.127 with standard errors exceeding the point estimates, and first-stage F-statistics collapse below the rule-of-thumb threshold of 10 in three of four specifications (minimum F=10.4, maximum F=32.4).

This pattern reveals that city size absorbs substantial variation in both historical densities (weakening the first stage) and contemporary pollution (affecting the reduced form), rendering the instrument uninformative once size is controlled. We interpret this as evidence that historical densities operate partly through the extensive margin of city growth (larger historical settlements became larger modern cities) rather than purely through intensive margin effects within cities of given size. This complicates the interpretation of our IV estimates: they capture the combined effect of within-city density gradients and between-city size differences, both predicted by historical settlement patterns. For policy purposes, this distinction matters: densification of existing cities versus urbanization into larger cities may have different pollution implications due to varying capacity for infrastructure adaptation. Given the weak instruments when controlling for city size, we do not claim our IV estimates isolate pure within-city density effects. Instead, they capture the total effect of urban concentration as historically determined —encompassing both neighborhood-level density and city-level scale— on pollution outcomes. This broader interpretation remains policy-relevant for evaluating urbanization trends but requires caution when extrapolating to pure densification scenarios.

6 Mechanisms

We develop a spatial equilibrium model of a monocentric city to characterize the mechanisms through which urban density and LEZs affect pollution exposure. The model extends the canonical Alonso-Muth-Mills framework (Alonso, 1964; Mills, 1967) by incorporating a pollution production function that depends on both distance to the CBD and residential density. This allows us to formalize the tradeoffs households face between accessibility, housing consumption, and pollution exposure, and to derive testable predictions about how LEZs alter these tradeoffs.

6.1 Setup

Consider a linear monocentric city represented by a segment on the positive real line. Production and consumption of a numéraire good take place at a single point $x = 0$, the CBD. The spatial extent of the city, denoted $\bar{x}$, is endogenously determined in equilibrium. Land covered by the city can be represented by the interval $[0, \bar{x}]$. There is a continuum of identical residents with total mass N. Each resident supplies one unit of labor inelastically at the CBD and earns a wage w. Residents choose where to live within the city and how to allocate their income between housing services h and a numéraire consumption good z. Preferences are represented by a utility function $u(h, z, p)$ that is increasing in housing and the numéraire, decreasing in pollution exposure p, and strictly quasi-concave in (h, z):

$$u(h, z, p) \text{ with } \frac{\partial u}{\partial h} > 0, \quad \frac{\partial u}{\partial z} > 0, \quad \frac{\partial u}{\partial p} < 0 \tag{11}$$

Commuting from residential location x to the CBD incurs a cost that increases linearly with distance at rate $\tau > 0$, so that total commuting cost is τx. This leaves $w - \tau x$ for expenditure on housing and the numéraire. Denoting by $P(x)$ the rental price of housing at distance x from the CBD, a resident living at location x faces the budget constraint:

$$w - \tau x = P(x)h + z. \tag{12}$$

A key departure from the standard monocentric model is that pollution exposure $p(x)$ varies across space and is determined endogenously by the spatial distribution of economic activity. We specify the pollution production function in Section 6.3, but for now we treat it as a general function $p(x)$ that residents take as given when making their location and consumption decisions. Housing is produced competitively from land and capital under constant returns to scale. The production function for housing delivers $f(R(x))$ units of housing floorspace per unit of land at location x, where $R(x)$ denotes the rental price of land and $f'(R(x)) > 0$. We denote the unit cost function in construction by $c(R(x))$, which is increasing in the land rent. All residents are freely mobile within the city and have identical preferences and income. Therefore, in equilibrium, all residents must achieve the same utility level $\bar{u}$, which we take as given (determined by the utility level available elsewhere in the economy in an open city framework). Land at the city edge $\bar{x}$ is available at an exogenous agricultural rent $\bar{R}$.

It is important to clarify which elements of the model are determined endogenously within the spatial equilibrium and which are taken as exogenous. The exogenous parameters are wage level w and commuting cost τ (transport technology), the pollution production function parameters φ and κ (defined in Section 6.3, the utility level $\bar{u}$ (open city assumption), agricultural land rent $\bar{R}$, total city population N (closed city) or endogenous if $\bar{u}$ is fixed (open city). The endogenous variables determined in equilibrium are housing price gradient $P(x)$, land price gradient $R(x)$, housing consumption $h(x)$, population density $n(x)$, pollution exposure $p(x)$ and city extent $\bar{x}$. These endogenous objects are determined simultaneously through the equilibrium conditions we derive below, reflecting the fundamental spatial general equilibrium nature of the model despite taking wages as given (a form of partial equilibrium with respect to the urban labor market).

6.2 Household Problem and Spatial Equilibrium

We solve for the spatial equilibrium using the bid-rent approach (Alonso, 1964), which provides the most direct path to characterizing the equilibrium price gradients. Define the bid-rent function for housing $\Psi(x, \bar{u})$ as the maximum price a resident is willing to pay for housing at distance x from the CBD while achieving utility $\bar{u}$ and satisfying the budget constraint:

$$\Psi(x, \bar{u}) \equiv \max_{h,z} \{P(x) \mid u(h, z, p(x)) = \bar{u},\ w - \tau x = P(x)h + z\} \tag{13}$$

This can be reformulated as an unconstrained problem by solving the budget constraint for $P(x)$ and substituting the restricted Hicksian demand for the numéraire $z(h, p(x), \bar{u})$:

$$\Psi(x, \bar{u}) = \max_h \left\{ \frac{w - \tau x - z(h, p(x), \bar{u})}{h} \right\} \tag{14}$$

The Alonso-Muth condition characterizing the equilibrium housing price gradient can be derived by applying the envelope theorem to equation (14):

$$\frac{dP(x)}{dx} = \left.\frac{d\Psi(x, \bar{u})}{dx}\right|_{h(x)=h(\Psi(x,\bar{u}),p(x),\bar{u})} = -\frac{\tau + \mathrm{MRS}_{p,z} \cdot \frac{dp(x)}{dx}}{h(x)}, \tag{15}$$

where $\mathrm{MRS}_{p,z} \equiv -\frac{\partial u/\partial p}{\partial u/\partial z} > 0$ is the marginal rate of substitution between pollution and the numéraire (the marginal willingness to pay for pollution reduction). Equation (15) is our pollution-augmented Alonso-Muth condition. It states that as a resident moves marginally farther from the CBD, the decrease in housing costs must exactly compensate for both (i) the increase in commuting costs τ and (ii) the change in pollution-induced disutility, valued at the marginal willingness to pay times the pollution gradient $\frac{dp(x)}{dx}$. When pollution is increasing with distance ($\frac{dp(x)}{dx} > 0$), the housing price gradient is steeper (more negative) than in the standard model without pollution. Conversely, if pollution decreases with distance ($\frac{dp(x)}{dx} < 0$), housing prices decline more gradually as distance from the CBD increases, since the pollution amenity partially offsets the commuting cost. As in the standard monocentric model, residents consume more housing as they move farther from the CBD. This follows from differentiating the Hicksian demand for housing:

$$\frac{dh(x)}{dx} = \frac{\partial h(P(x), p(x), \bar{u})}{\partial P(x)} \frac{dP(x)}{dx} + \frac{\partial h(P(x), p(x), \bar{u})}{\partial p(x)} \frac{dp(x)}{dx} \tag{16}$$

The first term is positive (lower housing prices induce greater housing consumption via a substitution effect), while the sign of the second term depends on whether housing and pollution are substitutes or complements in utility. If pollution disutility is separable in the utility function (i.e., $\frac{\partial^2 u}{\partial h \partial p} = 0$), the second term vanishes and housing consumption increases monotonically with distance. From the zero-profit condition in the competitive construction sector, $P(x) = c(R(x))$, we can relate the housing price gradient to the land price gradient:

$$\frac{dR(x)}{dx} = \frac{dP(x)}{dx} \cdot f(R(x)), \tag{17}$$

where $f(R(x)) = \frac{\partial c(R(x))}{\partial R(x)}$ by Shephard's lemma. Thus, the land rent gradient is proportional to the housing price gradient, with the proportionality factor equal to the capital-to-land ratio in construction.

6.3 Pollution Production Function

The pollution production function captures how ambient pollution at location x depends on the spatial structure of the city. We adopt a Cobb-Douglas specification:

$$p(x) = A \cdot x^{\varphi} \cdot n(x)^{\kappa}, \tag{18}$$

where $n(x)$ is the population density at location x, and $A > 0$ is a scaling parameter that captures background pollution levels or pollution from the CBD. The parameters φ and κ govern the elasticities of pollution with respect to distance and density, respectively. The functional form in equation (18) can be motivated by two sources of urban pollution:

1. Distance gradient ($\varphi < 0$): Pollution exposure typically decreases with distance from the CBD through two mechanisms. First, the CBD concentrates economic activity, generating high emissions from commercial buildings, industrial facilities, and convergent commuting flows that dissipate with distance through atmospheric dispersion. Second, population density declines with distance (as characterized in the equilibrium), reducing local emissions from residential heating and traffic. The power-law specification x^{φ} with $\varphi < 0$ captures this spatial decay: pollution levels are highest at the CBD and decline moving toward the urban periphery. The magnitude of $|\varphi|$ reflects the rate of spatial attenuation, which depends on wind patterns, topography, and the spatial distribution of emission sources. While commuting distances increase with x, this effect is typically dominated by the decline in emission source density, yielding net pollution decay.

2. Residential density emissions ($\kappa > 0$): Local pollution increases with population density through heating, local traffic congestion, and other density-related activities. The elasticity κ captures the degree of returns to density in pollution produc-

tion: $\kappa < 1$ implies decreasing returns (pollution grows sublinearly with density, perhaps due to scale economies in pollution abatement infrastructure), while $\kappa > 1$ implies increasing returns (congestion externalities dominate).

The multiplicative form $x^{\varphi} \cdot n(x)^{\kappa}$ allows the two sources to interact: for given density, pollution increases with distance (via commuting), and for given distance, pollution increases with density (via congestion). This interaction is empirically relevant, as dense central areas may have high pollution despite short commutes, while sparse peripheral areas may have high pollution from long commutes despite low density. Taking logs of equation (18) yields the empirical specification we estimate in Section 4:

$$\log p(x) = \log A + \varphi \log x + \kappa \log n(x). \tag{19}$$

This log-linear form provides the foundation for our identification strategy, where we estimate φ and κ from spatial variation in pollution and density, and analyze how these parameters change following the introduction of LEZs.

6.4 Characterization of Equilibrium

The spatial equilibrium is characterized by a system of differential equations that simultaneously determine the endogenous price and density gradients. Population density at each location is given by:

$$n(x) = \frac{f(R(x))}{h(x)}, \tag{20}$$

which states that density equals floorspace per unit of land divided by housing consumption per person. Combining equations (15), (17), and (20), we can express density in terms of the land price gradient:

$$n(x) = -\frac{1}{\tau + \mathrm{MRS}_{p,z} \cdot \frac{dp(x)}{dx}} \frac{dR(x)}{dx} \tag{21}$$

The city extent $\bar{x}$ is determined by the condition that land at the urban fringe is indifferent between urban and agricultural use:

$$R(\bar{x}) = \bar{R}. \tag{22}$$

Finally, the population constraint requires that the city accommodates the total population N:

$$\int_0^{\bar{x}} n(x)dx = N \tag{23}$$

The equilibrium is *partial* in the sense that we take wages w and the utility level $\bar{u}$ as given, abstracting from general equilibrium adjustments in the urban labor market. However, it is a spatial general equilibrium because all endogenous variables ($P(x)$, $R(x)$, $h(x)$, $n(x)$, $p(x)$, $\bar{x}$) are determined simultaneously through the interaction of household location choices and land markets. Pollution introduces an additional equilibrium feedback: higher density raises pollution (equation 18), which lowers the willingness to pay for housing (equation 15), which affects density (equation 20). This feedback is particularly important for understanding how LEZs, which alter the pollution production function, propagate through the spatial equilibrium.

6.5 Comparative Statics

We model a LEZ as a policy shock that affects the parameters governing pollution production and commuting costs within a designated area $[0, x_{\text{LEZ}}]$. Specifically, a LEZ can be represented as changing:

1. Commuting cost (τ): LEZs often involve access restrictions (e.g., bans on high-emission vehicles) or congestion charges that effectively increase the monetary cost of commuting by private vehicle: $\tau \to \tau^{\text{LEZ}} > \tau$ for $x \in [0, x_{\text{LEZ}}]$.

2. Distance-pollution gradient (φ): By reducing pollution emissions within the LEZ (particularly from the concentrated sources in the CBD), LEZs flatten the spatial pollution gradient. Since $\varphi < 0$ in the baseline (pollution declines with distance from CBD), an effective LEZ should make this gradient less steep: $\varphi^{\text{LEZ}} > \varphi$ (i.e., less negative) for $x \in [0, x_{\text{LEZ}}]$. This reflects that LEZs disproportionately reduce pollution near emission sources in the central city, narrowing the gap between central and peripheral pollution levels.

3. Density-pollution elasticity (κ): LEZs may alter the relationship between density and pollution through two channels: (a) mode substitution toward less polluting but less spatially efficient modes (public transport, walking, cycling) increases κ, or

(b) adoption of cleaner heating/energy technologies decreases κ. The net effect is theoretically ambiguous: $\kappa \to \kappa^{\text{LEZ}}$ with sign to be determined empirically.

The impact on density is ambiguous. Higher commuting costs discourage peripheral residence, increasing central density. However, lower pollution in the LEZ increases the willingness to pay for central locations, which could either amplify density (if housing supply is elastic) or simply capitalize into higher prices (if supply is inelastic). The change in κ directly affects how density translates into pollution, creating an additional feedback loop. A crucial feature of our empirical setting is the presence of spillover effects to areas outside the LEZ boundary, $x > x_{\text{LEZ}}$. The sign and magnitude of these spillovers are theoretically ambiguous, as the LEZ generates effects through multiple competing channels. Some channels generating positive spillovers (pollution reduction outside LEZ) are:

1. Network effects: Reduced traffic volumes within the LEZ may decrease congestion on arterial roads and highways that pass through or near the LEZ, benefiting areas outside the boundary. If total vehicle-kilometers traveled in the city decline (e.g., through mode substitution or trip suppression), this reduces pollution both inside and outside the LEZ.

2. Technology adoption spillovers: The LEZ creates incentives for vehicle fleet upgrading (e.g., purchasing cleaner vehicles to maintain access). Households living near but outside the LEZ boundary may upgrade their vehicles for convenience, even if not legally required, generating positive technology spillovers. Similarly, firms operating delivery or service vehicles may upgrade their entire fleets rather than maintaining separate vehicles for LEZ vs. non-LEZ routes.

3. Modal shift complementarities: Improved public transport infrastructure within the LEZ (often accompanying LEZ policies) may serve residents in adjacent areas, enabling mode substitution that reduces pollution beyond the formal LEZ boundary.

4. Reduced through-traffic: If the LEZ deters vehicles from entering the city center, this may reduce pollution along commuting routes in peripheral areas, particularly if drivers avoid the city altogether or shift to alternative routes with lower total emissions.

We also could observe channels generating negative spillovers (pollution increase outside LEZ):

1. Relocation spillovers: If the LEZ increases commuting costs or reduces amenities within $[0, x_{\text{LEZ}}]$ (through congestion from modal shifts or other mechanisms), households may relocate to areas just outside the LEZ. This increases density $n(x)$ in the spillover zone, which by equation (18) increases pollution there even though φ and κ remain unchanged outside the LEZ.

2. Traffic diversion: Vehicles seeking to avoid LEZ restrictions or charges may divert to routes that circumvent the zone, increasing traffic (and hence pollution) on peripheral roads. This channel operates through an effective increase in the commuting emissions parameter for non-LEZ routes.

3. Displacement of dirty vehicles: If the LEZ displaces older, higher-emission vehicles rather than inducing their retirement, these vehicles may concentrate in areas outside the LEZ, increasing local pollution there.

The net spillover effect depends on which channels dominate. If network effects, technology adoption, and modal shift complementarities are strong, we expect *positive spillovers* (pollution reduction outside the LEZ), consistent with the LEZ generating city-wide benefits beyond its formal boundary. Conversely, if relocation and traffic diversion dominate, we expect *negative spillovers* (pollution increase outside the LEZ), with the policy partially displacing rather than eliminating pollution. Thus, our theoretical framework yields several predictions that we can test using our spatial panel dataset:

Prediction 1 ***(Pollution-Density Gradient)*** *In cities without LEZs, pollution should increase with residential density with elasticity $\kappa > 0$, and decrease with distance from the CBD with elasticity $\varphi < 0$ (equation 19).*

Prediction 2 ***(LEZ Effect on Pollution)*** *LEZs should reduce pollution within the designated zone through both direct effects (flatter spatial gradient, i.e., $\varphi^{LEZ} > \varphi$, less negative) and indirect effects (density adjustments responding to changing τ and pollution levels).*

Prediction 3 ***(Parameter Shifts)*** *Post-LEZ, we should observe:*

- *Flatter distance-pollution gradient:* $\varphi^{LEZ} > \varphi$ *(less negative, indicating LEZs reduce the spatial pollution gradient by disproportionately lowering central pollution)*

- *Changed density-pollution elasticity:* $\kappa^{LEZ} \neq \kappa$ *(sign depends on dominant channel: mode substitution vs. technology adoption)*

- *Steeper housing price gradient near CBD if* $\tau^{LEZ} > \tau$ *(though this requires hedonic price data we do not have)*

Prediction 4 ***(Ambiguous Spillovers)*** *The sign of spillover effects to areas adjacent to the LEZ boundary is theoretically ambiguous:*

- *Negative spillovers (pollution reduction at* xx_{LEZ}*): If network effects, technology adoption, and modal complementarities dominate, pollution decreases both within the LEZ and in adjacent areas.*

- *Positive spillovers (pollution increase at* xx_{LEZ}*): If relocation and traffic diversion dominate, pollution decreases within the LEZ, but increases in adjacent areas as activity and traffic are displaced.*

The empirical sign of spillovers reveals which channels are quantitatively more important. Negative spillovers suggest the LEZ generates city-wide benefits through network effects and technology diffusion, while positive spillovers indicate displacement effects dominate.

Prediction 5 ***(Aggregate Exposure)*** *The net effect on city-wide pollution exposure depends on the relative magnitudes of the within-LEZ reduction and the spillover increase, weighted by population distribution. If population is concentrated within the LEZ, aggregate exposure falls even with positive spillovers.*

These predictions guide our empirical strategy in Sections 4 and 6, where we estimate the parameters (φ, κ) and their changes following LEZ implementation, and quantify the within-zone and spillover effects.

6.6 Empirical Validation: Estimating the Pollution Production Function

Having established the theoretical predictions of our pollution production function, we now test whether the data support the key functional form assumptions embodied in equation (18). Specifically, we estimate the reduced-form relationship between pollution, distance to the CBD (proxied by distance to LEZ boundaries), and population density, and examine whether these elasticities shift following LEZ implementation as predicted by the comparative statics. Table 11 presents estimates from the following specification:

$$\log p_{it} = \varphi \cdot \log(\mathrm{x})_{it} + \kappa \cdot \log(\mathrm{n(x)})_{it} + \varphi^{\Delta} \cdot \log(\mathrm{x})_{it} \times \mathrm{Post}_{it} + \kappa^{\Delta} \cdot \log(\mathrm{n(x)})_{it} \times \mathrm{Post}_{it} + \alpha_c + \gamma_t + \varepsilon, \tag{24}$$

where i indexes grid cells, t indexes years, γ_t are year fixed effects and c are city fixed effects. The coefficients φ and κ capture the baseline (pre-LEZ) elasticities of pollution with respect to distance and density, while φ^{Δ} and κ^{Δ} measure how these elasticities change post-LEZ implementation. Columns (1)-(2) restrict to cities with single LEZs to avoid treatment interference, while columns (3)-(4) expand to all cities in our dataset. Even-numbered columns add weather controls (temperature, wind speed, precipitation, distance to closest water form, power plants location and ruggedness).

Table 11: Pollution Production Function: Distance and Density Elasticities

	(1)	(2)	(3)	(4)
Log(Distance to LEZ)	-0.003**	-0.003***	-0.002***	-0.002***
	(0.001)	(0.001)	(0.0004)	(0.0004)
Log(Density)	0.028	0.029	0.013*	0.013*
	(0.019)	(0.019)	(0.007)	(0.007)
Log(Distance) × Post	0.002**	0.002**	0.002***	0.002***
	(0.001)	(0.0010)	(0.0004)	(0.0004)
Log(Density) × Post	-0.011	-0.012	-0.001	-0.001
	(0.012)	(0.012)	(0.005)	(0.005)
Year	Yes	Yes	Yes	Yes
City	Yes	Yes	Yes	Yes
Observations	54,935	54,935	235,568	235,568
R^2	0.71706	0.71874	0.79456	0.79902
Within R^2	0.04492	0.05059	0.03185	0.05287

Dependent variable: log(PM2.5). Columns (1)-(2) restrict to cities with single LEZ. Columns (3)-(4) include all cities in sample. All specifications include year and city fixed effects. Spatially robust (Conley at 3km) standard errors. The interaction terms test whether distance-pollution (φ) and density-pollution (κ) elasticities change post-LEZ implementation.

The baseline distance-pollution elasticity φ is negative and statistically significant in all specifications, ranging from -0.002 to -0.003. This confirms Prediction 1: pollution decreases with distance from the CBD, consistent with the spatial decay of emission sources and atmospheric dispersion. The magnitude implies that a 10% increase in distance from the LEZ boundary is associated with a 0.02-0.03% reduction in PM2.5 concentrations. While economically modest, this gradient is precisely estimated and robust to sample composition and control variables. The baseline density-pollution elasticity κ is positive and highly significant, ranging from 0.013 in the full sample to 0.028 in the single-LEZ sample. This validates the second component of Prediction 1: pollution increases with population density through congestion, heating, and other density-related emissions. Notably, these within-city elasticities are substantially smaller than the between-cities elasticity of 0.06 estimated in Section 4, suggesting that spatial variation within cities reflects more efficient density: areas that are dense within a given city tend to have better public transport infrastructure, walkability, and economies of scale in pollution abatement relative to comparable density levels achieved by simply comparing across cities of different sizes. In the Cobb-Douglas pollution production function framework (equation 18), this implies that the total factor productivity parameter A varies systematically with city characteristics —larger, more established cities have lower A (cleaner production of urban services) conditional on density, absorbing some of the pollution that would otherwise arise from agglomeration. The larger elasticity in the single-LEZ sample may reflect that these cities have more severe congestion or less efficient pollution abatement infrastructure relative to the broader sample.

The interaction term $\log(\text{Distance}) \times \text{Post}$ is positive and significant (0.002, p¡0.10 in most specifications), suggesting the distance-pollution gradient flattens post-LEZ: the elasticity becomes less negative ($\varphi^{\text{LEZ}} = \varphi + \varphi^{\Delta} = -0.003 + 0.002 = -0.001$). This represents a 67% reduction in the magnitude of the spatial gradient, indicating that LEZs substantially compress the pollution differential between central and peripheral areas. While the baseline gradient implies pollution falls 0.03% per 10% increase in distance pre-LEZ, this decay rate drops to just 0.01% post-LEZ, consistent with Prediction 3 that LEZs disproportionately reduce pollution near emission sources in the CBD. However, the modest magnitude and marginal significance indicate this spatial flattening channel, while directionally correct, is quantitatively secondary to the direct pollution reductions documented in our main results.

The interaction term $\log(\text{n(x)}) \times \text{Post}$ is consistently negative but statistically insignificant, ranging from -0.001 to -0.011 across specifications. This null result indicates the density-pollution elasticity κ remains stable following LEZ adoption: the technological relationship governing how population concentration translates into pollution intensity is unchanged by the policy. In the context of equation (18), this means LEZs operate by reducing the productivity parameter A (shifting-down the entire pollution production function) rather than altering the returns to density κ. The stability of κ validates our pollution production function specification and confirms that LEZ effects work through reducing emission rates per capita or per vehicle rather than fundamentally restructuring urban density patterns or the density-pollution technology. This finding complements our main results: if LEZs primarily worked through displacing economic activity from treated to untreated areas, we would expect spatial reallocation to change how density generates pollution. The absence of such changes reinforces the fleet renewal interpretation over spatial displacement. This interpretation seems to be confirmed with available data on registered vehicles of different technologies coinciding with the introduction of LEZs in European cities.

7 Conclusion

This paper provides the first systematic continental-scale evaluation of LEZ effectiveness in Europe, explicitly accounting for spatial spillovers and documenting the pollution-density elasticity that governs how urban agglomeration generates environmental externalities. Four main findings emerge from our analysis.

First, LEZ adoption reduces population-weighted PM2.5 exposure by approximately 4% within designated zones, with robust evidence of positive spillovers extending to areas 1-3km beyond LEZ boundaries. These spillover effects—pollution reductions of 2.2% in adjacent areas—indicate that network effects and technology adoption spillovers dominate displacement mechanisms in practice. The spatial decay pattern we document is consistent with fleet renewal being the primary channel through which LEZs operate: vehicle upgrades induced by access restrictions benefit not only trips within the LEZ but also journeys throughout the metropolitan area. Aggregating across spatial zones weighted by population distribution, we estimate that LEZs reduce city-wide pollution exposure by approximately 1.8%, representing a meaningful public health improvement despite being substantially smaller than the within-zone effect.

Second, the pollution-density elasticity in European cities is approximately 0.06, implying that a 1% increase in experienced density raises PM2.5 exposure by 6%. This elasticity is remarkably stable across specifications, instruments, and spatial scales, and is approximately half the magnitude documented for US cities using comparable methods. The lower European elasticity suggests that differences in urban form -more compact cities with steeper density gradients-, transport systems with higher public transit mode shares, and industrial composition with less heavy manufacturing within city boundaries, moderate the environmental costs of agglomeration relative to North America. This cross-continental difference has important implications for urban policy: European cities can accommodate higher densities with smaller pollution penalties than their US counterparts, strengthening the case for densification as a sustainable growth strategy.

Third, our spatial equilibrium model clarifies the mechanisms through which LEZs affect pollution exposure. By formalizing the pollution production function as depending on both distance to the CBD (capturing commuting emissions) and residential density (capturing congestion externalities), the model generates testable predictions about LEZ impacts and spillover signs. Our empirical validation confirms that pollution exhibits spatial decay from the CBD (distance elasticity $\phi \approx -0.003$) and increases with density (elasticity $\kappa \approx 0.028$ within cities), consistent with the model's predictions. Critically, the distance-pollution gradient flattens post-LEZ implementation, indicating that LEZs disproportionately reduce central pollution, while the density-pollution elasticity remains stable, confirming that fleet renewal rather than spatial displacement drives observed effects.

Fourth, substantial heterogeneity exists in LEZ effectiveness across city characteristics and policy design. Larger cities and those with medium-sized LEZ coverage relative to total urban area exhibit stronger treatment effects, likely reflecting better enforcement capacity and optimal spatial targeting. Our estimate of a 4% average reduction across diverse European contexts (while smaller than the 19% effect documented for Madrid Central) reflects the typical policy implementation rather than the upper bound achievable under ideal conditions. This distinction is crucial for policy evaluation: our results provide realistic benchmarks for what cities can expect from LEZ adoption under normal enforcement and compliance conditions, while cases like Madrid Central demonstrate the potential of particularly aggressive interventions. Because effects are concentrated in larger and denser cities, the average reduction we report may overstate the benefits LEZs deliver in small or low-density urban areas, a caveat policymakers should weigh before extending the instrument beyond major metropolitan centres.

Fifth, our treatment indicator captures LEZ adoption but not the design margin (the stringency of vehicle restrictions and the intensity of enforcement), which varies widely across our sample; a harmonised, cross-country measure of enforcement would allow the average effect we report to be decomposed by policy design.

These findings have several implications for urban environmental policy. First, LEZ policies deliver net environmental benefits even when implemented with moderate stringency, as positive spillovers ensure aggregate exposure reductions exceed within-zone effects. Policymakers concerned about displacement can take reassurance from our consistent evidence that LEZs do not merely redistribute pollution spatially. Second, the fleet renewal mechanism we identify suggests that LEZ effectiveness will strengthen over time as non-compliant vehicles age out of the stock, implying that the medium-run effects (3-5 years post-implementation) documented here may understate long-run benefits. Third, the lower pollution-density elasticity in European cities relative to the US indicates that European urban form and transport systems provide a partial buffer against agglomeration-driven pollution, though substantial environmental costs of density remain. Fourth, the substantial heterogeneity we document in LEZ effectiveness underscores that policy design matters: cities considering LEZ adoption should prioritize comprehensive spatial coverage, stringent vehicle restrictions, and robust enforcement mechanisms to maximize pollution reductions.

Our analysis has several limitations that suggest directions for future research. First, we focus exclusively on PM2.5 concentrations, the most health-relevant pollutant, but LEZs may have differential effects on other pollutants (NO_2, ozone) or on noise pollution and traffic congestion. Extending our spatial framework to these outcomes would provide a more complete picture of LEZ impacts. Second, our welfare analysis is partial: we quantify pollution reductions but do not estimate the costs borne by households and firms complying with restrictions, the benefits from reduced mortality and morbidity, or the distributional impacts across income groups and neighborhoods. A full cost-benefit analysis would require integrating our pollution estimates with epidemiological dose-response functions, vehicle upgrade costs, and hedonic valuation of environmental amenities. Third, our theoretical model abstracts from dynamic adjustments in housing supply, industrial location, and urban spatial structure that may unfold over longer horizons than our 15-year panel captures. Structural estimation of the model's parameters would enable counterfactual simulations of alternative LEZ designs and provide guidance for optimal spatial targeting. Fourth, we cannot directly observe most of the mechanisms driving our results -mode choice, trip suppression- limiting our ability to decompose the treatment effect into its constituent channels. Linking our geospatial pollution data with vehicle registration records, traffic counts, and transit ridership would enable more granular mechanism analysis. In particular, matching our panel to city-level transport-infrastructure measures – such as the stock of dedicated cycling lanes or bus-rapid-transit coverage – would allow a direct test of the modal-shift complementarity channel we hypothesise.

Despite these limitations, our findings make clear that LEZs represent an effective policy instrument for reducing urban air pollution in European cities, generating city-wide benefits through fleet renewal and network effects that extend well beyond their formal boundaries. As European cities continue to grapple with the challenge of reconciling urban agglomeration's productivity benefits with its environmental costs, LEZs offer a targeted intervention that meaningfully reduces pollution exposure while allowing cities to maintain the density necessary for economic dynamism.

References

Ahlfeldt, Gabriel M., and Elisabetta Pietrostefani. (2019). "The economic effects of density: A synthesis". *Journal of Urban Economics*, 111, pp. 93-107. https://doi.org/10.1016/j.jue.2019.04.006

Alonso, William. (1964). *Location and Land Use: Toward a General Theory of Land Rent*. Harvard University Press. https://doi.org/10.4159/harvard.9780674730854

Anderson, Michael L. (2019). "As the wind blows: The effects of long-term exposure to air pollution on mortality". *Journal of the European Economic Association*, 18(4), pp. 1886-1927. https://doi.org/10.1093/jeea/jvz051

Balboni, Clare, and Joseph S. Shapiro. (2025). "Spatial environmental economics". NBER Working Paper Series, 33377, National Bureau of Economic Research. https://doi.org/10.3386/w33377

Banzhaf, Spencer, Lala Ma and Christopher Timmins. (2019). "Environmental justice: The economics of race, place, and pollution". *Journal of Economic Perspectives*, 33(1), pp. 185-208. https://doi.org/10.1257/jep.33.1.185

Bernardo, Valeria, Xavier Fageda and Ricardo Flores-Fillol. (2021). "Pollution and congestion in urban areas: The effects of low emission zones". *Economics of Transportation*, 26-27(100221). https://doi.org/10.1016/j.ecotra.2021.100221

Blackman, Allen, Francisco Alpízar, Fredrik Carlsson and Marisol Rivera Planter. (2018). "A contingent valuation approach to estimating regulatory costs: Mexico's day without driving program". *Journal of the Association of Environmental and Resource Economists*, 5(3), pp. 607-641. https://doi.org/10.1086/697416

Blackman, Allen, Ping Qin and Jun Yang. (2020). "How costly are driving restrictions? Contingent valuation evidence from Beijing". *Journal of Environmental Economics and Management*, 104(102366). https://doi.org/10.1016/j.jeem.2020.102366

Borck, Rainald, and Philipp Schrauth. (2021). "Population density and urban air quality". *Regional Science and Urban Economics*, 86(103596). https://doi.org/10.1016/j.regsciurbeco.2020.103596

Borck, Rainald, and Philipp Schrauth. (2022). "Urban pollution: A global perspective". CESifo Working Paper Series, 10171, CESifo. https://EconPapers.repec.org/RePEc:ces:ceswps:_10171

Borusyak, Kirill, Xavier Jaravel and Jann Spiess. (2024). "Revisiting event-study designs: Robust and efficient estimation". *The Review of Economic Studies*, 91(6), pp. 3253-3285. https://doi.org/10.1093/restud/rdae007

Burchfield, Marcy, Henry G. Overman, Diego Puga and Matthew A. Turner. (2006). "Causes of sprawl: A portrait from space". *The Quarterly Journal of Economics*, 121(2), pp. 587-633. https://doi.org/10.1162/qjec.2006.121.2.587

Burnett, Richard, Hong Chen, Mieczysław Szyszkowicz, Neal Fann, Bryan Hubbell, C. Arden Pope III, Joshua S. Apte, Michael Brauer, Aaron Cohen, Scott Weichenthal, Jay Coggins, Qian Di, Bert Brunekreef, Joseph Frostad, Stephen S. Lim, Haidong Kan, Katherine D. Walker, George D. Thurston, Richard B. Hayes, Chris C. Lim, ... Joseph V. Spadaro. (2018). "Global estimates of mortality associated with long-term exposure to out-door fine particulate matter". *Proceedings of the National Academy of Sciences*, 115(38), pp. 9592-9597. https://doi.org/10.1073/pnas.1803222115

Butts, Kyle. (2023). "Difference-in-differences estimation with spatial spillovers". https://arxiv.org/abs/2105.03737

Callaway, Brantly, and Pedro H. C. Sant'Anna. (2021). "Difference-in-differences with multiple time periods". *Journal of Econometrics*, 225(2), pp. 200-230. https://doi.org/10.1016/j.jeconom.2020.12.001

Carozzi, Felipe, and Sefi Roth. (2023). "Dirty density: Air quality and the density of American cities". *Journal of Environmental Economics and Management*, 118(102767). https://doi.org/10.1016/j.jeem.2022.102767

Ciccone, Antonio, and Robert E. Hall. (1993). "Productivity and the density of economic activity". NBER Working Paper Series, 4313, National Bureau of Economic Research. https://doi.org/10.3386/w4313

Combes, Pierre-Philippe, Gilles Duranton and Laurent Gobillon. (2011). "The identification of agglomeration economies". *Journal of Economic Geography*, 11(2), pp. 253-266. https://doi.org/10.1093/jeg/lbq038

Combes, Pierre-Philippe, Gilles Duranton, Laurent Gobillon and Sébastien Roux. (2010). "Chapter 1 Estimating Agglomeration Economies with History, Geology, and Worker Effects". In Edward L. Glaeser (ed.), *Agglomeration economics*. University of Chicago Press, pp. 15-66. https://doi.org/10.7208/chicago/9780226297927.003.0002

Commission, European, and Eurostat. (2021). *Applying the degree of urbanisation – A methodological manual to define cities, towns and rural areas for international comparisons – 2021 edition*. Publications Office of the European Union. https://doi.org/10.2785/706535

Cornes, Richard C., Gerard van der Schrier, Else J. M. van den Besselaar and Philip D. Jones. (2018). "An ensemble version of the E-OBS temperature and precipitation data sets". *Journal of Geophysical Research: Atmospheres*, 123(17), pp. 9391-9409. https://doi.org/10.1029/2017JD028200

De Chaisemartin, Clément, and Xavier d'Haultfoeuille. (2020). "Two-way fixed effects estimators with heterogeneous treatment effects". *American Economic Review*, 110(9), pp. 2964-2996. https://doi.org/10.1257/aer.20181169

Duranton, Gilles, and Diego Puga. (2020). "The economics of urban density". *Journal of Economic Perspectives*, 34(3), pp. 3-26. https://doi.org/10.1257/jep.34.3.3

Duranton, Gilles, and Stuart S. Rosenthal. (2021). "Special issue on delineation of urban areas". *Journal of Urban Economics*, 125-S(103352). https://doi.org/10.1016/j.jue.2021.103352

Duscher, Klaus, and Andreas Günther. (2019). *Extended vector data of the international hydrogeological map of Europe 1:1,500,000* (version ihme1500 v1.2) [Dataset]. BGR Technical Note, Federal Institute for Geosciences and Natural Resources. https://www.bgr.bund.de/EN/Themen/Grundwasser/Projekte/Flaechen-Rauminformationen/Ihme1500/ihme1500-v12_technical-note.pdf?__blob=publicationFile&v=3

European Environment Agency. (2023). *Harm to human health from air pollution in Europe: Burden of disease 2023*. Briefing, 23/2023, European Environment Agency. https://doi.org/10.2800/721439

Galdon-Sanchez, Jose Enrique, Ricard Gil, Felix Holub and Guillermo Uriz-Uharte. (2023). "Social benefits and private costs of driving restriction policies: The impact of Madrid Central on congestion, pollution, and consumer spending". *Journal of the European Economic Association*, 21(3), pp. 1227-1267. https://doi.org/10.1093/jeea/jvac064

Global Energy Observatory. (2018). *Global power plant database* (csv) [Dataset]. KTH Royal Institute of Technology in Stockholm Enipedia World Resources Institute, Google Earth Engine.

Goldewijk, C.G.M. Klein. (2017). *Anthropogenic land-use estimates for the Holocene; HYDE 3.2* (v2) [Dataset]. DANS Data Station Archaeology. https://doi.org/10.17026/dans-25g-gez3

Goldewijk, Kees Klein, Arthur Beusen, Jonathan Doelman and Elke Stehfest. (2017). "Anthropogenic land use estimates for the Holocene – HYDE 3.2". *Earth System Science Data*, 9(2), pp. 927-953. https://doi.org/10.5194/essd-9-927-2017

Goodman-Bacon, Andrew. (2021). "Difference-in-differences with variation in treatment timing". *Journal of econometrics*, 225(2), pp. 254-277. https://doi.org/10.1016/j.jeconom.2021.03.014

Graff Zivin, Joshua, and Matthew Neidell. (2012). "The impact of pollution on worker productivity". *American Economic Review*, 102(7), pp. 3652-3673. https://doi.org/10.1257/aer.102.7.3652

Hanna, Rema, and Paulina Oliva. (2015). "The effect of pollution on labor supply: Evidence from a natural experiment in Mexico City". *Journal of Public Economics*, 122, pp. 68-79. https://doi.org/10.1016/j.jpubeco.2014.10.004

Heblich, Stephan, Alex Trew and Yanos Zylberberg. (2021). "East-side story: Historical pollution and persistent neighborhood sorting". *Journal of Political Economy*, 129(5), pp. 1508-1552. https://doi.org/10.1086/713101

Henderson, J. Vernon, Dzhamilya Nigmatulina and Sebastian Kriticos. (2021). "Measuring urban economic density". *Journal of Urban Economics*, 125S(103188). https://doi.org/10.1016/j.jue.2019.103188

IIASA, FAO. (2023). *Harmonized world soil database* (v2.0) [Dataset]. International Institute for Applied Systems Analysis. https://www.fao.org/soils-portal/data-hub/soil-maps-and-databases/harmonized-world-soil-database-v20/en/

Leape, Jonathan. (2006). "The London congestion charge". *Journal of Economic Perspectives*, 20(4), pp. 157-176. https://doi.org/10.1257/jep.20.4.157

Mills, Edwin S. (1967). "An aggregative model of resource allocation in a metropolitan area". *The American Economic Review*, 57(2), pp. 197-210. Papers and Proceedings of the Seventy-ninth Annual Meeting of the American Economic Association. https://www.jstor.org/stable/1821621

Nunn, Nathan, and Diego Puga. (2012). "Ruggedness: The Blessing of Bad Geography in Africa". *The Review of Economics and Statistics*, 94(1), pp. 20-36. https://doi.org/10.1162/REST_a_00161

Roca, Jorge De La, and Diego Puga. (2017). "Learning by working in big cities". *The Review of Economic Studies*, 84(1), pp. 106-142. https://doi.org/10.1093/restud/rdw031

Schmidheiny, Kurt, and Sebastian Siegloch. (2023). "On event studies and distributed-lags in two-way fixed effects models: Identification, equivalence, and generalization". *Journal of Applied Econometrics*, 38(5), pp. 695-713. https://doi.org/10.1002/jae.2971

Sims, Kelly, Andrew Reith, Edward Bright, Jason Kaufman, Joe Pyle, Justin Epting, Jack Gonzales, Daniel Adams, Eric Powell, Marie Urban and Amy Rose. (2023). *LandScan global 2022* (csv) [Data set]. Oak Ridge National Laboratory.

Wolff, Hendrik. (2014). "Keep your clunker in the suburb: Low-emission zones and adoption of green vehicles". *The Economic Journal*, 124(578), pp. F481-F512. https://doi.org/10.1111/ecoj.12091

A Appendix

A.1 Figures

Figure 6: Spatial Distribution of Population

Notes: Data for 2019. The figure is plotted for Albania, Austria, Belgium, Bulgaria, Croatia, Cyprus, Czechia, Denmark, Estonia, Finland, France, Germany, Greece, Hungary, Iceland, Ireland, Italy, Latvia, Lithuania, Montenegro, Netherlands, North Macedonia, Norway, Poland, Portugal, Romania, Serbia, Slovakia, Slovenia, Spain, Sweden, Switzerland and United Kingdom using data as in section 2. For more info about the data, please consult section 2.

Figure 7: Spatial Distribution of PM2.5

Notes: Data for 2019. The figure is plotted for Albania, Austria, Belgium, Bulgaria, Croatia, Cyprus, Czechia, Denmark, Estonia, Finland, France, Germany, Greece, Hungary, Iceland, Ireland, Italy, Latvia, Lithuania, Montenegro, Netherlands, North Macedonia, Norway, Poland, Portugal, Romania, Serbia, Slovakia, Slovenia, Spain, Sweden, Switzerland and United Kingdom using data as in section 2. For more info about the data, please consult section 2.

A.2 Descriptives

A.3 Regressions

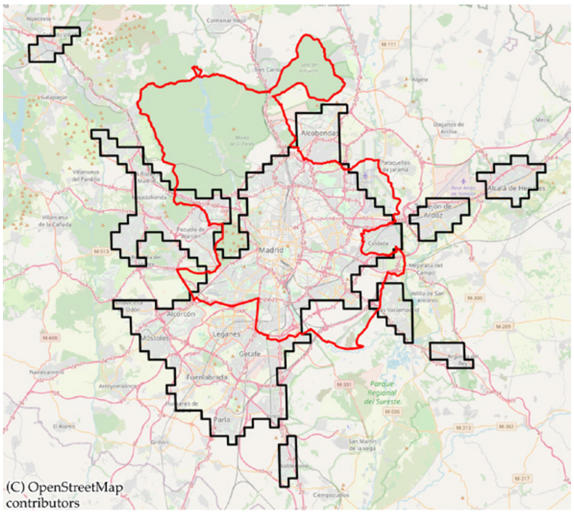

Figure 8: Madrid administrative vs. **our** delineation

Figure 9: Pollution Trends Around LEZ Implementation

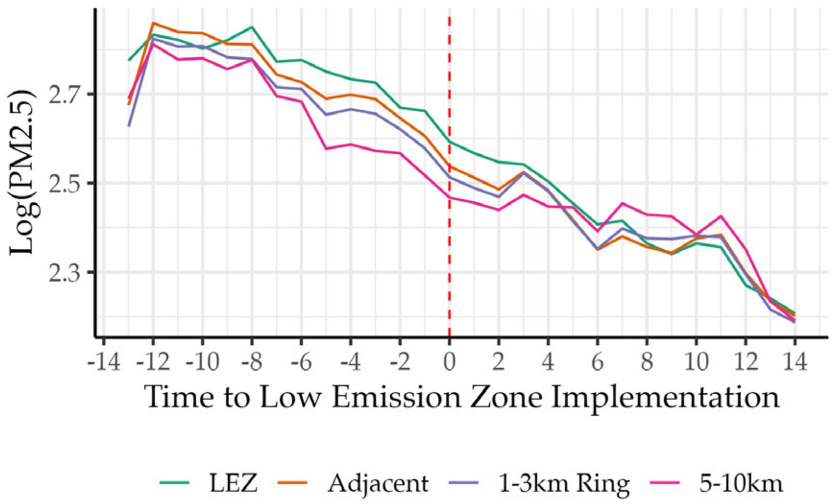

Notes: Average log PM2.5 by years relative to LEZ implementation. Sample includes 66 LEZ-adopting cities, 2007-2022. Each line represents mean pollution for cells in the specified zone: LEZ (green) = cells within LEZ boundary; Adjacent (orange) = 0-1km from boundary; 1-3km Ring (purple) = 1-3km from boundary; 5-10km (pink) = control cells, between the 5-10km from LEZ zone. Vertical dashed line marks LEZ implementation (time = 0). Pre-treatment period shows parallel trends across all zones, validating the identifying assumption. Post-treatment divergence indicates heterogeneous spatial effects.

Figure 10: Urban Areas with Multiple LEZs

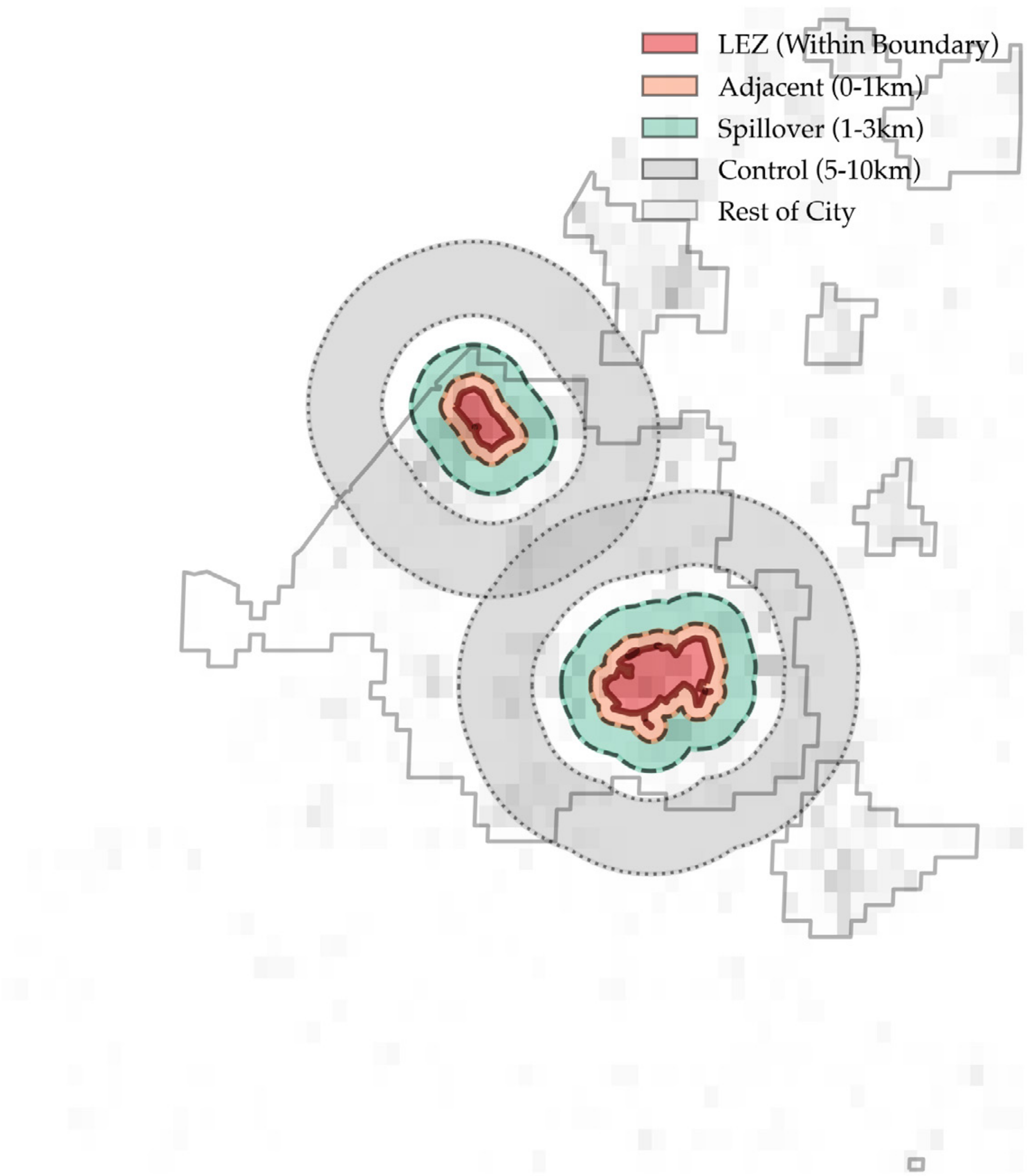

Notes: Ambient population in 2020 (LandScan). This figure illustrates the challenge of treatment interference in cities with multiple LEZs, using the Rotterdam-The Hague metropolitan area in the Netherlands as an example. Both cities implemented separate LEZs (red zones) with overlapping buffer zones: the control zone (5-10km, gray) of one LEZ intersects with the spillover zone (1-3km, teal) of the other. This spatial overlap violates the Stable Unit Treatment Value Assumption (SUTVA), as cells designated as ”control” for one LEZ are simultaneously ”treated” by spillover effects from the neighboring LEZ. To avoid such contamination, our main analysis restricts to cities with a single LEZ only and a minimum 10% control group size (relative to city size). Cities with multiple LEZs like Rotterdam-The Hague are excluded from the baseline sample but included in robustness checks that account for treatment interference.

Table 12: Descriptive Statistics of Cities instruments (between)

	Mean	Standard Deviation
Population in 100 A.D.	0.10	0.61
Population in 1000 A.D.	0.13	0.79
Population in 1500 A.D.	0.43	1.94
Population in 1800 A.D.	1.47	5.23
Highly productive porous aquifers	0.31	0.38
Low and moderately productive porous aquifers	0.22	0.34
Highly productive fissured aquifers	0.11	0.25
Low and moderately productive fissured aquifers	0.08	0.23
Locally aquiferous rocks, porous or fissured	0.18	0.31
Practically non-aquiferous rocks, porous or fissured	0.10	0.24

Notes: Population is expressed in millions of people. Aquifer variables measure the share of land withn a city with such aquifer characteristic. Yearly (2007-2022) averages and standard deviation for Albania, Austria, Belgium, Bulgaria, Croatia, Cyprus, Czechia, Denmark, Estonia, Finland, France, Germany, Greece, Hungary, Iceland, Ireland, Italy, Latvia, Lithuania, Montenegro, Netherlands, North Macedonia, Norway, Poland, Portugal, Romania, Serbia, Slovakia, Slovenia, Spain, Sweden, Switzerland and United Kingdom . Population and experienced density is expressed in millions of persons, temperature in Celsius degrees, precipitation in millimiters per day, wind speed in meters per second (in thousands) at a 10 meter height above the surface, and all distance variables are expressed in kilometers (km).

Table 13: Cities Soil Quality: Share of Land by Quality

	Excess Salts	Nutrient availability	Nutrient retention	Oxygen availability	Rooting conditions	Toxicity	Workability
Mainly non-soil	0.02	0.03	0.02	0.02	0.02	0.02	0.02
Moderate limitations	0.24	0.24	0.21	0.24	0.24	0.24	0.24
No or slight limitations	0.48	0.50	0.57	0.48	0.48	0.48	0.48
Sever limitations	0.13	0.13	0.09	0.13	0.13	0.13	0.13
Very severe limitations	0.07	0.05	0.04	0.07	0.07	0.07	0.07

Notes: Yearly Averages (2007 - 2022) for Albania, Austria, Belgium, Bulgaria, Croatia, Cyprus, Czechia, Denmark, Estonia, Finland, France, Germany, Greece, Hungary, Iceland, Ireland, Italy, Latvia, Lithuania, Montenegro, Netherlands, North Macedonia, Norway, Poland, Portugal, Romania, Serbia, Slovakia, Slovenia, Spain, Sweden, Switzerland and United Kingdom .

Table 14: Robustness: CS Estimates Across Time Windows

	Main $[-8,+8]$	Long All Years	Short $[-5,+5]$
Panel A: LEZ Zone			
	-0.069***	-0.049***	-0.027***
	(0.005)	(0.005)	(0.003)
Panel B: Adjacent Zone (0-1km)			
	-0.023***	-0.003	-0.015***
	(0.006)	(0.007)	(0.005)
Panel C: Spillover Zone (1-3km)			
	-0.009*	0.011**	-0.011***
	(0.004)	(0.004)	(0.004)

Notes: This table presents CS estimates across different time windows to assess robustness. Column 1 reproduces main specification from Table 2 using time window $[-8,+8]$ years relative to LEZ implementation. Column 2 uses all available years (2007-2022) without time restrictions. Column 3 restricts to narrow window $[-5,+5]$ years. Results qualitatively consistent across specifications, confirming findings are not driven by specific time windows. Standard errors clustered at cell level. *** p<0.01, ** p<0.05, * p<0.10.

Table 15: Robustness: TWFE with Long Time Window

	(1)	(2)	(3)
LEZ × Post	-0.023***	-0.005	-0.025*
	(0.009)	(0.014)	(0.013)
Adjacent	-0.021**	-0.020**	-0.020**
	(0.009)	(0.009)	(0.009)
Spillover 1-3km	-0.016*	-0.015*	-0.014*
	(0.008)	(0.008)	(0.008)
Year	Yes	Yes	Yes
Cell	Yes	Yes	Yes
Observations	155,632	112,640	116,000
Adjusted R^2	0.92631	0.93105	0.93092

Notes: This table presents TWFE estimates using all available years (2007-2022) without time window restrictions. Column 1: all cities with interference. Column 2: single LEZ cities only. Column 3: adds restriction on control group size (>=10% of city area). Results qualitatively consistent with main specification. Conley (3km) standard errors in parentheses. *** p<0.01, ** p<0.05, * p<0.10.

Table 16: Robustness: TWFE with Short Time Window

	(1)	(2)	(3)
LEZ × Post	-0.022**	-0.024*	-0.036***
	(0.009)	(0.012)	(0.011)
Adjacent	-0.020**	-0.019**	-0.019**
	(0.009)	(0.009)	(0.009)
Spillover 1-3km	-0.015*	-0.014*	-0.014*
	(0.008)	(0.008)	(0.008)
Year	Yes	Yes	Yes
Cell	Yes	Yes	Yes
Observations	134,191	106,149	108,336
Adjusted R^2	0.92958	0.93445	0.93449

Notes: This table presents TWFE estimates using restricted time window $[-5, +5]$ years relative to LEZ implementation. Column structure identical to main specification. Tighter time window ensures comparison across more similar time periods. Results qualitatively consistent with main specification. Conley (3km) standard errors in parentheses. *** p<0.01, ** p<0.05, * p<0.10.

Table 17: Between OLS Estimates for PM2.5 Exposure

	(1)	(2)	(3)	(4)	(5)	(6)
Log(Population)	0.034***		0.033***		0.030***	
	(0.003)		(0.003)		(0.004)	
Log(Exp. Density)		0.017***		0.030***		0.048***
		(0.004)		(0.003)		(0.009)
Country					Yes	Yes
Year					Yes	Yes
All Controls	No	No	Yes	Yes	Yes	Yes
Observations	13,008	13,008	13,008	13,008	13,008	13,008

Notes: Signif. Codes: ***: 0.01, **: 0.05, *: 0.1. Clustered (country and year) standard-errors in parentheses. Fixed Effects: Country and year. Temporal coverage: 2007-2022. Countries: Albania, Austria, Belgium, Bulgaria, Croatia, Cyprus, Czechia, Denmark, Estonia, Finland, France, Germany, Greece, Hungary, Iceland, Ireland, Italy, Latvia, Lithuania, Montenegro, Netherlands, North Macedonia, Norway, Poland, Portugal, Romania, Serbia, Slovakia, Slovenia, Spain, Sweden, Switzerland and United Kingdom .

Table 18: Within OLS Estimates for Population Density

	25km Buffer	Only Cities	25km Buffer	Only Cities	25km Buffer	Only Cities
Log (Population)	0.033***	0.022***	0.046***	0.020***	0.045***	0.022***
	(0.0005)	(0.002)	(0.0005)	(0.001)	(0.0003)	(0.0008)
Fixed-effects						
Country					Yes	Yes
Year					Yes	Yes
Fit statistics						
Observations	18,417,179	1,091,775	18,417,179	1,091,775	18,417,179	1,091,775
Adjusted R^2	0.028	0.010	0.204	0.321	0.712	0.771

Notes: Signif. Codes: ***: 0.01, **: 0.05, *: 0.1. Spatially (3km) robust, Conley standard-errors in parentheses. Fixed Effects: Country and year. Temporal coverage: 2007-2022. Countries: Albania, Austria, Belgium, Bulgaria, Croatia, Cyprus, Czechia, Denmark, Estonia, Finland, France, Germany, Greece, Hungary, Iceland, Ireland, Italy, Latvia, Lithuania, Montenegro, Netherlands, North Macedonia, Norway, Poland, Portugal, Romania, Serbia, Slovakia, Slovenia, Spain, Sweden, Switzerland and United Kingdom . . Columns 1, 3 and 5 take a 25km buffer for each city, so that 25km rural areas outside the city are also included in the sample.

Table 19: Between Cities PM2.5 Exposure IV Estimates with Population Density

Model:	(1)	(2)	(3)	(4)	(5)	(6)	(7)	(8)	(9)	(10)	(11)	(12)
Log(Pop.)	0.041***	0.041***	0.041***	0.041***	0.035***	0.036***	0.035***	0.035***	0.130	0.124	0.125	0.121
Observations	13,008	13,008	13,008	13,008	13,008	13,008	13,008	13,008	13,008	13,008	13,008	13,008
Adjusted R^2	0.786	0.788	0.791	0.791	0.787	0.789	0.791	0.791	0.710	0.722	0.723	0.729
F-test (1st stage)	125.9	125.6	125.6	125.6	6,238.3	6,236.3	6,251.2	6,252.2	16.6	15.6	15.8	15.7
Wu-Hausman	22.2	21.0	21.0	20.6	6.92	8.84	7.84	7.43	36.0	29.8	31.2	28.5
Log (Exp. dens.)	0.052***	0.055***	0.055***	0.055***	0.062***	0.063***	0.063***	0.063***	0.033	0.073	0.085	0.081
	(0.010)	(0.010)	(0.009)	(0.009)	(0.013)	(0.011)	(0.010)	(0.010)	(0.106)	(0.118)	(0.116)	(0.118)
Observations	13,008	13,008	13,008	13,008	13,008	13,008	13,008	13,008	13,008	13,008	13,008	13,008
Adjusted R^2	0.789	0.792	0.794	0.794	0.788	0.791	0.793	0.793	0.789	0.790	0.789	0.790
F-test (1st stage)	103.4	103.9	104.2	104.2	3,155.6	3,158.0	3,180.8	3,178.3	19.0	18.5	18.4	18.2
Wu-Hausman	1.85	3.08	3.47	3.47	14.3	13.5	13.2	12.7	0.425	1.31	2.82	2.19
Weather	Yes	Yes	Yes	Yes	Yes	Yes	Yes	Yes	Yes	Yes	Yes	Yes
Geological		Yes	Yes	Yes		Yes	Yes	Yes		Yes	Yes	Yes
Water			Yes	Yes			Yes	Yes			Yes	Yes
Power Plants				Yes				Yes				Yes
Fixed-effects												
country and year	Yes	Yes	Yes	Yes	Yes	Yes	Yes	Yes	Yes	Yes	Yes	Yes

Notes: Signif. Codes: ***: 0.01, **: 0.05, *: 0.1. Clustered (country and year) standard-errors in parentheses. Fixed Effects: country and year. Temporal coverage: 2007-2022. Countries: Albania, Austria, Belgium, Bulgaria, Croatia, Cyprus, Czechia, Denmark, Estonia, Finland, France, Germany, Greece, Hungary, Iceland, Ireland, Italy, Latvia, Lithuania, Montenegro, Netherlands, North Macedonia, Norway, Poland, Portugal, Romania, Serbia, Slovakia, Slovenia, Spain, Sweden, Switzerland and United Kingdom.

Table 20: PM2.5 Exposure IV Estimates Robustness: Historical Densities

	100 AD	1000 AD	1500 AD	1800 AD
Log (Experienced Density)	0.076***	0.079***	0.072***	0.063***
	(0.018)	(0.012)	(0.011)	(0.010)
Observations	13,008	13,008	13,008	13,008
Adjusted R^2	0.791	0.791	0.792	0.793
F-test (1st stage), $\log_d ens_e xp$	1,566.6	1,604.8	2,353.2	3,178.3
Wu-Hausman	23.0	28.6	25.7	12.7
Weather	Yes	Yes	Yes	Yes
Geological	Yes	Yes	Yes	Yes
Water	Yes	Yes	Yes	Yes
Power Plants	Yes	Yes	Yes	Yes
FE: Country and year	Yes	Yes	Yes	Yes

Notes: Signif. Codes: ***: 0.01, **: 0.05, *: 0.1. Clustered (country and year) standard-errors in parentheses. Fixed Effects: Country and year. Temporal coverage: 2007-2022. Countries: Albania, Austria, Belgium, Bulgaria, Croatia, Cyprus, Czechia, Denmark, Estonia, Finland, France, Germany, Greece, Hungary, Iceland, Ireland, Italy, Latvia, Lithuania, Montenegro, Netherlands, North Macedonia, Norway, Poland, Portugal, Romania, Serbia, Slovakia, Slovenia, Spain, Sweden, Switzerland and United Kingdom .

Table 21: Robustness Check for Between Cities PM2.5 Exposure IV Estimates using Multiple Soil Quality Specifications

	(1)	(2)	(3)	(4)	(5)	(6)	(7)
Incrementally							
Log (Exp. Dens)	0.071***	0.060***	0.059***	0.059***	0.059***	0.056***	0.055***
	(0.010)	(0.010)	(0.010)	(0.010)	(0.010)	(0.010)	(0.009)
F-test (1st stage)	614.3	319.9	219.7	170.5	138.7	119.7	104.2
Separately							
Log (Exp. Dens)	0.071***	0.063***	0.060***	0.063***	0.056***	0.045**	0.068***
	(0.010)	(0.015)	(0.015)	(0.014)	(0.012)	(0.015)	(0.011)
F-test (1st stage)	614.3	499.8	477.1	432.8	426.4	410.2	590.0
Weather	Yes	Yes	Yes	Yes	Yes	Yes	Yes
Geological	Yes	Yes	Yes	Yes	Yes	Yes	Yes
Water	Yes	Yes	Yes	Yes	Yes	Yes	Yes
Power Plants	Yes	Yes	Yes	Yes	Yes	Yes	Yes
Fixed-effects	Yes	Yes	Yes	Yes	Yes	Yes	Yes
Observations	13,008	13,008	13,008	13,008	13,008	13,008	13,008

Columns 1 to 7 stand for different soil characteristics (ordered): toxicity, nutrient retention, nutrient availability, workability, rooting conditions and excess of salts. *Notes:* Signif. Codes: ***: 0.01, **: 0.05, *: 0.1. Clustered (country and year) standard-errors in parentheses. Fixed Effects: Country and year. Temporal coverage: 2007-2022. Countries: Albania, Austria, Belgium, Bulgaria, Croatia, Cyprus, Czechia, Denmark, Estonia, Finland, France, Germany, Greece, Hungary, Iceland, Ireland, Italy, Latvia, Lithuania, Montenegro, Netherlands, North Macedonia, Norway, Poland, Portugal, Romania, Serbia, Slovakia, Slovenia, Spain, Sweden, Switzerland and United Kingdom .

Table 22: Robustness Check in Between Cities PM2.5 Exposure IV Estimates for City Size adding City Area

	No Polynomial	Sum Population	2nd Degree Pol	3rd Degree Pol
City Area: ***NO***				
Log (Exp. Dens)	0.065***	0.056	0.012	0.004
	(0.008)	(0.103)	(0.096)	(0.179)
F-test (1st stage)	472.4	25.1	32.0	15.5
City Area: ***YES***				
Log (Exp. Dens)	0.085	0.041	0.028	0.127
	(0.120)	(0.082)	(0.095)	(0.222)
F-test (1st stage)	16.5	32.4	30.3	10.4
Weather	Yes	Yes	Yes	Yes
Geological	Yes	Yes	Yes	Yes
Water	Yes	Yes	Yes	Yes
Power Plants	Yes	Yes	Yes	Yes
Fixed Effects	Yes	Yes	Yes	Yes
Observations	13,008	13,008	13,008	13,008

Notes: Signif. Codes: ***: 0.01, **: 0.05, *: 0.1. Clustered (country and year) standard-errors in parentheses. Fixed Effects: Country and year. Temporal coverage: 2007-2022. Countries: Albania, Austria, Belgium, Bulgaria, Croatia, Cyprus, Czechia, Denmark, Estonia, Finland, France, Germany, Greece, Hungary, Iceland, Ireland, Italy, Latvia, Lithuania, Montenegro, Netherlands, North Macedonia, Norway, Poland, Portugal, Romania, Serbia, Slovakia, Slovenia, Spain, Sweden, Switzerland and United Kingdom . . Column (1) shows adds no polynomial terms of population, column (2) adds the sum of population of a given city, and the following columns add a squared and cubic exponential terms to the sum of population to the control covariates.

Table 23: Within Cities PM2.5 Exposure IV Estimates

	25km Buffer	Only Cities	25km Buffer	Only Cities	25km Buffer	Only Cities
Log(Pop.)	0.089***	0.071***	0.076***	0.066***	0.199***	0.046***
	(0.002)	(0.005)	(0.001)	(0.006)	(0.004)	(0.009)
Weather						
Geological	Yes	Yes	Yes	Yes	Yes	Yes
Water	Yes	Yes	Yes	Yes	Yes	Yes
Power Plants	Yes	Yes	Yes	Yes	Yes	Yes
FE	Yes	Yes	Yes	Yes	Yes	Yes
Observations	18,417,179	1,091,775	18,417,179	1,091,775	18,417,179	1,091,775
F-test (1st stage), $log_{p}op_{r}as$	42,961.9	2,156.9	2,841,968.7	67,569.6	58,355.6	1,371.2
Wu-Hausman	205,951.9	14,653.1	235,002.2	11,968.9	711,530.6	445.5

Notes: Signif. Codes: ***: 0.01, **: 0.05, *: 0.1. Spatially (3km) robust, Conley standard-errors in parentheses. Fixed Effects: Country and year. Temporal coverage: 2007-2022. Countries: Albania, Austria, Belgium, Bulgaria, Croatia, Cyprus, Czechia, Denmark, Estonia, Finland, France, Germany, Greece, Hungary, Iceland, Ireland, Italy, Latvia, Lithuania, Montenegro, Netherlands, North Macedonia, Norway, Poland, Portugal, Romania, Serbia, Slovakia, Slovenia, Spain, Sweden, Switzerland and United Kingdom .

BANCO DE ESPAÑA PUBLICATIONS

WORKING PAPERS

2510 PETER KARADI, ANTON NAKOV, GALO NUÑO, ERNESTO PASTÉN and DOMINIK THALER: Strike while the Iron is Hot: Optimal Monetary Policy with a Nonlinear Phillips Curve.

2511 MATTEO MOGLIANI and FLORENS ODENDAHL: Density forecast transformations.

2512 LUCÍA LÓPEZ, FLORENS ODENDAHL, SUSANA PÁRRAGA and EDGAR SILGADO-GÓMEZ: The pass-through to inflation of gas price shocks.

2513 CARMEN BROTO and OLIVIER HUBERT: Desertification in Spain: Is there any impact on credit to firms?

2514 ANDRÉS ALONSO-ROBISCO, JOSÉ MANUEL CARBÓ, PEDRO JESÚS CUADROS-SOLAS and JARA QUINTANERO: The effects of open banking on fintech providers: evidence using microdata from Spain.

2515 RODOLFO G. CAMPOS and JACOPO TIMINI: Trade bloc enlargement when many countries join at once.

2516 CORINNA GHIRELLI, JAVIER J. PÉREZ and DANIEL SANTABÁRBARA: Inflation and growth forecast errors and the sacrifice ratio of monetary policy in the euro area.

2517 KOSUKE AOKI, ENRIC MARTORELL and KALIN NIKOLOV: Monetary policy, bank leverage and systemic risk-taking.

2518 RICARDO BARAHONA: Index fund flows and fund distribution channels.

2519 ALVARO FERNÁNDEZ-GALLARDO, SIMON LLOYD and ED MANUEL: The Transmission of Macroprudential Policy in the Tails: Evidence from a Narrative Approach.

2520 ALICIA AGUILAR: Beyond fragmentation: unraveling the drivers of yield divergence in the euro area.

2521 RUBÉN DOMÍNGUEZ-DÍAZ and DONGHAI ZHANG: The macroeconomic effects of unemployment insurance extensions: A policy rule-based identification approach.

2522 IRMA ALONSO-ALVAREZ, MARINA DIAKONOVA and JAVIER J. PÉREZ: Rethinking GPR: The sources of geopolitical risk.

2523 ALBERTO MARTÍN, SERGIO MAYORDOMO and VICTORIA VANASCO: Banks vs. Firms: Who Benefits from Credit Guarantees?

2524 SUMIT AGARWAL, SERGIO MAYORDOMO, MARÍA RODRÍGUEZ-MORENO and EMANUELE TARANTINO: Household Heterogeneity and the Lending Channel of Monetary Policy.

2525 DIEGO BONELLI, BERARDINO PALAZZO, and RAM YAMARTHY: Good inflation, bad inflation: implications for risky asset prices.

2526 STÉPHANE BONHOMME and ANGELA DENIS: Fixed Effects and Beyond. Bias Reduction, Groups, Shrinkage and Factors in Panel Data.

2527 ÁLVARO FERNÁNDEZ-GALLARDO and IVÁN PAYÁ: Public debt burden and crisis severity.

2528 GALO NUÑO: Three Theories of Natural Rate Dynamics.

2529 GALO NUÑO, PHILIPP RENNER and SIMON SCHEIDEGGER: Monetary policy with persistent supply shocks.

2530 MIGUEL ACOSTA-HENAO, MARÍA ALEJANDRA AMADO, MONTSERRAT MARTÍ and DAVID PÉREZ-REYNA: Heterogeneous UIPDs across Firms: Spillovers from U.S. Monetary Policy Shocks.

2531 LUIS HERRERA and JESÚS VÁZQUEZ: Learning from news.

2532 MORTEZA GHOMI, JOCHEN MANKART, RIGAS OIKONOMOU and ROMANOS PRIFTIS: Debt maturity and government spending multipliers.

2533 MARINA DIAKONOVA, CORINNA GHIRELLI and JAVIER J. PÉREZ: Political polarization in Europe.

2534 NICOLÁS FORTEZA and SERGIO PUENTE: Measuring non-workers' labor market attachment with machine learning.

2535 GERGELY GANICS and LLUC PUIG CODINA: Simple Tests for the Correct Specification of Conditional Predictive Densities.

2536 HENRIQUE S. BASSO and OMAR RACHEDI: Robot adoption and inflation dynamics.

2537 PABLO GARCIA, PASCAL JACQUINOT, ČRT LENARČIČ, KOSTAS MAVROMATIS, NIKI PAPADOPOULOU and EDGAR SILGADO-GÓMEZ: Green transition in the Euro area: domestic and global factors.

2538 MARÍA ALEJANDRA AMADO, CARLOS BURGA and JOSÉ E. GUTIÉRREZ: Cross-border spillovers of bank regulations: Evidence of a trade channel.

2539 ALEJANDRO CASADO and DAVID MARTÍNEZ-MIERA: Banks' specialization and private information.

2540 CHRISTIAN E. CASTRO, ÁNGEL ESTRADA GARCÍA and GONZALO FERNÁNDEZ DIONIS: Diversifying sovereign risk in the Euro area: empirical analysis of different policy proposals.

2541 RAFAEL GUNTIN and FEDERICO KOCHEN: The Origins of Top Firms.

2542 ÁLVARO FERNÁNDEZ-GALLARDO: Natural disasters, economic activity, and property insurance: evidence from weekly U.S. state-level data.

2543 JOSÉ ELÍAS GALLEGOS, ESTEBAN GARCÍA-MIRALLES, IVÁN KATARYNIUK and SUSANA PÁRRAGA RODRÍGUEZ: Fiscal Announcements and Households' Beliefs: Evidence from the Euro Area.

2544 LUIS HERRERA, MARA PIROVANO and VALERIO SCALONE: From risk to buffer: Calibrating the positive neutral CCyB rate.

2545 ESTEBAN GARCÍA-MIRALLES et al.: Fiscal drag in theory and in practice: A European perspective.

2546 TATSURO SENGA and IACOPO VAROTTO: Investment Irreversibility in a Granular World.

2547 OLYMPIA BOVER, NEZIH GUNER, YULIYA KULIKOVA, ALESSANDRO RUGGIERI and CARLOS SANZ: Family-friendly policies and fertility: What firms have to do with it?

2548 ADINA-ELENA FUDULACHE and MARIA DEL CARMEN CASTILLO LOZOYA: Demand drivers of central bank liquidity: A time-to-exit TLTRO analysis.

2549 ERIK ANDRES-ESCAYOLA, LUIS MOLINA, JAVIER J. PÉREZ and ELENA VIDAL: How economic policy uncertainty spreads across borders: the case of Latin America.

2550 MATTHIAS BURGERT, MATTHIEU DARRACQ PARIÈS, LUIGI DURAND, MARIO GONZÁLEZ, ROMANOS PRIFTIS, OKE RÖHE, MATTHIAS ROTTNER, EDGAR SILGADO-GÓMEZ, NIKOLAI STÄHLER and JANOS VARGA: Macroeconomic effects of carbon-intensive energy price changes: A model comparison.

2601 IACOPO VAROTTO: Blocking the Blockers? Diversity Matters.

2602 CARLOS CAÑIZARES MARTÍNEZ, ADRIANA LOJSCHOVÁ and ALICIA AGUILAR: Non-linear effects of monetary policy shocks on housing: Evidence from a CESEE country.

2603 DIEGO BONELLI: Inflation risk and yield spread changes.

2604 MARÍA ALEJANDRA AMADO: Macroprudential FX Regulations and Small Firms: Unintended Consequences for Credit Growth.

2605 FERNANDO ÁVALOS, BORIS HOFMANN and JOSE M. SERENA: Monetary policy and private equity acquisitions: tracing the links.

2606 RICARD GREBOL, MARGARITA MACHELETT, JAN STUHLER and ERNESTO VILLANUEVA: Assortative Mating, Inequality, and Rising Educational Mobility in Spain.

2607 PABLO AGUILAR, RUBÉN DOMÍNGUEZ-DÍAZ, JOSÉ-ELÍAS GALLEGOS and JAVIER QUINTANA: The Transmission of Foreign Shocks in a Networked Economy.

2608 ERWAN GAUTIER, CRISTINA CONFLITTI, DANIEL ENDERLE, LUDMILA FADEJEVA, ALEX GRIMAUD, EDUARDO GUTIÉRREZ, VALENTIN JOUVANCEAU, JAN-OLIVER MENZ, ALARI PAULUS, PAVLOS PETROULAS, PAU ROLDAN-BLANCO and ELISABETH WIELAND: Consumer price stickiness in the euro area during an inflation surge.

2609 MORTEZA GHOMI and SAMUEL HURTADO: RAUI: Uncertainty Indicators Built With Artificial Intelligence.

2610 MORTEZA GHOMI and EVI PAPPA: Stimulating avenues: EIB loans and returns to Public Investment.

2611 JUAN S. MORA-SANGUINETTI, CRISTINA PEÑASCO and ROK SPRUK: The impact of "Green Regulation" on firms' innovation.

2612 ÁLVARO FERNÁNDEZ-GALLARDO and EVI PAPPA: Natural disasters and fiscal shelters.

2613 NICOLÁS BONINO-GAYOSO and MÓNICA CORREA-LÓPEZ: Unexpecting the expected in real-time inflation forecasting: The inflation expectations channel?

2614 ANDRÉS AZQUETA-GAVALDÓN, MARINA DIAKONOVA, CORINNA GHIRELLI and JAVIER J. PÉREZ: Diverging signals from economic uncertainty measures: Uncovering coherence through news narratives.

2615 JOSÉ E. GUTIÉRREZ, ENRIC MARTORELL and MARIYA MELNYCHUK: The nexus between the deposit and risk-taking channels of monetary policy.

2616 MARTA GARCÍA-RODRÍGUEZ and CLEMENTE PINILLA-TORREMOCHA: The role of confidence measures in European unemployment dynamics.

2617 DANIEL DEJUAN-BITRIA: Processing forward-looking loan loss provisions: evidence from the adoption of the CECL model.

2618 RYAN BANERJEE, FRANCISCO GONZÁLEZ, JOSÉ E. GUTIÉRREZ and JOSE-MARÍA SERENA: Credit Supply in the Wake of Distressed Bank Acquisitions.

2619 ALEJANDRO CASADO, MARCO GIOMETTI, JOSÉ E. GUTIÉRREZ, DAVID MARTÍNEZ-MIERA, ALEXANDRA MATYUNINA and TAMMARO TERRACCIANO: Digitalization and credit markets: Evidence from e-Invoicing.

2620 JORGE ABAD, SAKI BIGIO, SALOMÓN GARCÍA-VILLEGAS, JOËL MARBET and GALO NUÑO: The Heterogeneous Bank Lending Channel of Monetary Policy.

2621 NICOLÁS FORTEZA and JOSÉ M. LABEAGA: Pollution, Density and Low Emission Zones: European Evidence.